

**UCSF**

**UC San Francisco Electronic Theses and Dissertations**

**Title**

Conformational transitions in designed peptides

**Permalink**

<https://escholarship.org/uc/item/9hw5c5gk>

**Author**

Cerpa, Robert K.

**Publication Date**

1995

Peer reviewed|Thesis/dissertation

Conformational Transitions in Designed Peptides

by

Robert K. Cerpa

**DISSERTATION**

**Submitted in partial satisfaction of the requirements for the degree of**

**DOCTOR OF PHILOSOPHY**

**in**

Biophysics

**in the**

**GRADUATE DIVISION**

**of the**

**UNIVERSITY OF CALIFORNIA**

**San Francisco**



## ACKNOWLEDGEMENTS

This work would have been impossible were it not for the generous support of many people. First and foremost, I want to thank Tack Kuntz, my thesis advisor, for his unwavering support, constant encouragement, and perpetual optimism. Tack has my admiration not only as a superlative scientist, but also as a human being of great wisdom and compassion. Julie Ransom has also been a rock of stability in sometimes stormy seas. Her good humor and gentle nature has smoothed the way for many a Biophysics student, and her prodigious efforts on behalf of myself and all the members of the Graduate Group in Biophysics are much appreciated.

Professor Fred Cohen has provided much scientific and personal guidance, for which I am thankful. Professor Tom James has been helpful and supportive throughout my time at UCSF. I thank both professors for reading my thesis.

Several members and associates of the Kuntz lab have given freely of their time and expertise. Dr. Erin Bradley, whose good cheer was always a breath of fresh air, helped get me up and running in the lab. Professors Phyllis Kosen and Vladimir Basus provided me with invaluable experimental assistance. The computer expertise of Mark Day and Don Kneller was essential to the NMR lab. And Dennis Benjamin's ready wit, joviality and deep thoughts were always inspiring.

I owe thanks to many other members of UCSF. Simon Friedman, Eric Pettersen, Chris Schafmeister, Diana Roe, Elaine Meng, and Wendy Cornell have been the best friends one could hope for. Karen Han's gentle grace has always been a source of support. The generous assistance of Dallas Connor and Professor Martin Shetlar is gratefully acknowledged, as is the irrepressible enthusiasm of our labmate Yoko Shibata Haga.

The Howard Hughes Medical Institute Predoctoral Fellowship program provided me with financial support for five years, and my sixth year in graduate school was paid for by a University of California President's Year Dissertation Fellowship. I thank HHMI and UC for the funding.

Finally, I wish to express my appreciation for the love and support of my parents, Matilda J. Cerpa and Ted P. Cerpa. They taught me to love knowledge and to seek to use it for the benefit of humanity. Whatever success I achieve in life, I owe to them, and whatever good I accomplish springs from their guidance.

# Conformational Switching in Designed Peptides

Robert K. Cerpa

## ABSTRACT

Understanding why particular secondary structures form from a primary sequence is critical to a complete description of protein structure. In this work we examine two *de novo* designed peptides which display alpha helix to beta sheet conformational transitions under a variety of solution conditions. Changes in pH, salt concentration, temperature, or peptide concentration all affect the conformation which the peptides will adopt. One peptide contains the photoisomerizable artificial amino acid, p-phenylazo-L-phenylalanine, and displays a beta sheet to alpha helix transition upon UV irradiation.

The transitions are explained by postulating a multimeric beta sheet and a monomeric alpha helix. Solution conditions that tend to favor aggregation--higher peptide concentration, pH values where the peptide is neutral, higher salt concentrations at pH values where the peptide is charged--cause the peptide to display spectra characteristic of beta sheet. Conversely, solution conditions that tend to disfavor aggregation cause the display of characteristic helical spectra. Biological ramifications and spectroscopic considerations are discussed.

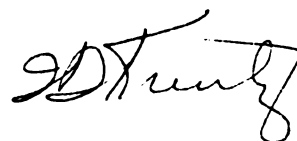


## TABLE OF CONTENTS

INTRODUCTION.....	1
Relating Sequence to Structure.....	2
Switch Peptides.....	7
Azobenzene Switch Peptides.....	8
Biological Implications of Switch Peptides.....	10
Peptide Chemistry.....	11
Circular Dichroism.....	14
Infrared Spectroscopy.....	17
Nuclear Magnetic Resonance.....	18
Design of Peptides Used in this Study.....	19
EXPERIMENTAL.....	27
Synthesis of Fmoc-p-phenylazo-L-phenylalanine.....	27
Peptide Synthesis.....	30
Circular Dichroism.....	35
Fourier-Transform Infrared Spectroscopy.....	38
Ultraviolet Irradiation.....	40
Nuclear Magnetic Resonance Spectroscopy.....	41
RESULTS.....	42
pH Titration.....	42
Salt Concentration Effects.....	50
Temperature Effects.....	54
Concentration Effects.....	60
Photoisomerization Effects.....	61
Nuclear Magnetic Resonance Spectra.....	63
DISCUSSION.....	73
Nature of the Structural States.....	73
Significance of the Conformational Transition.....	80
Spectroscopic Considerations.....	82
Conclusions.....	84
REFERENCES.....	86
APPENDIX.....	94

## LIST OF TABLES

**Table I.** Resonance Assignments of Peptide I.....70

**Table II.** Resonance Assignments of Peptide II ( $> 0.05$  ppm  $\Delta\delta$  from peptide I).....71

## LIST OF FIGURES

Figure 1: Trans, cis forms of azobenzene.....	9
Figure 2: Sequences of peptides used in this study.....	20
Figure 3: Peptide I in antiparallel beta-sheet conformation...	22
Figure 4: Peptide II in model beta sheet conformation.....	23
Figure 5: Peptide II in model alpha helix conformation.....	24
Figure 6: Mass spectrum of purified peptide I.....	33
Figure 7: Mass spectrum of purified peptide II.....	34
Figure 8: HPLC trace of purified peptide I.....	36
Figure 9: HPLC trace of purified peptide II.....	37
Figure 10: Peptide I pH titration, 100 $\mu$ M peptide conc.....	42
Figure 11: Peptide I pH titration, 100 $\mu$ M peptide conc.....	43
Figure 12: Peptide I pH titration, 1.2 mM peptide conc.....	44
Figure 13: Peptide I pH titration, 1.2 mM peptide conc.....	45
Figure 14: "Reverse" peptide I pH titration.....	46
Figure 15: "Reverse" peptide I pH titration.....	47
Figure 16: "Reverse" peptide I pH titration.....	48
Figure 17: Peptide II pH titration, 870 $\mu$ M peptide conc.....	49
Figure 18: Peptide II CD curves, with and without salt.....	50
Figure 19: Peptide II salt titration.....	51
Figure 20: FTIR spectrum of peptide II.....	52
Figure 21: FTIR spectrum of peptide II, with, without NaCl....	53
Figure 22: Temperature denaturation CD curves, peptide II...54	
Figure 23: Temperature denaturation CD curves, peptide II...55	
Figure 24: Time course of peptide II CD heating curves.....	56
Figure 25: Time course of peptide II CD heating curves.....	57
Figure 26: Time course of peptide II CD heating curves.....	58
Figure 27: Time course of peptide II CD heating curves.....	59
Figure 28: Peptide II dilution CD curves.....	60
Figure 29: Peptide II before and after UV irradiation.....	61
Figure 30: Time course of peptide II irradiation curves.....	62
Figure 31: NOESY spectrum of peptide I, fingerprint region...64	
Figure 32: NOESY spectrum of peptide I, amide region.....	65
Figure 33: Summary of NOEs, peptide I.....	66
Figure 34: NOESY spectrum of peptide II, fingerprint region...67	
Figure 35: NOESY spectrum of peptide II, amide region.....	68
Figure 36: Summary of NOEs, peptide II.....	69



## **INTRODUCTION**

Understanding the principles of protein structure is an essential prerequisite for understanding protein function. A detailed description of critical protein functions, such as enzyme catalysis, receptor specificity, and DNA regulation, must include an accounting of how the protein structure interacts with other molecules. The amino acid main chain of proteins can form alpha helices, beta sheets, turns, and irregular structures. Elucidating the rules of protein architecture could be simplified if each of these elements could be studied in isolation, and if the lessons learned from such basic studies on the individual elements of structure could be combined to understand the structure of the overall protein.

Emil Fischer perceived the importance of structure to function; this formed the basis of his "lock-and-key" hypothesis of 1894 (Fersht, 1985). An atomic-level description of structural patterns in proteins was developed by Linus Pauling. His recognition that hydrogen bonding would play an important role in protein structure enabled him to predict the structure of the alpha-helix and beta-sheet components of proteins (Pauling and Corey, 1951; Pauling et al., 1951). Pauling's predictions were borne out when the first three-dimensional protein structures were solved, the crystal structures of myoglobin and hemoglobin as determined by X-ray diffraction (Lesk, 1991). Anfinsen's classic experiment on the refolding of ribonuclease A demonstrated that, at least in some cases, the primary structure of

a protein could specify the tertiary structure which that protein adopts (Anfinsen et al., 1961).

## **Relating Sequence to Structure**

Anfinsen's experiments led to intense efforts to relate primary and tertiary structure, with the relationship between primary and secondary structure being a necessary intermediate step en route. Early experimental efforts aimed at understanding the influence of sequence on secondary structure were carried out by Scheraga (Scheraga, 1978). Because homopolymers of many amino acids are insoluble, Scheraga utilized a water-soluble homopolymer (e.g. polyhydroxypropylglutamine) which has a well-characterized transition between alpha helix and random coil. By preparing random copolymers of an individual naturally-occurring amino acid (the "guest") with the water-soluble amino acid (the "host"), Scheraga's "host-guest" experiments enabled him to construct a scale for the tendencies of each amino acid to stabilize or destabilize the helical behavior of the resulting heteropolymer. These tendencies could be expressed using the parameters  $\sigma$  and  $s$  of the Zimm-Bragg helix-coil theory (Zimm and Bragg, 1959). Scheraga's work led to the important--and, in retrospect, incorrect!--conclusions that the difference in the helix-forming tendencies of the amino acids was slight, and that short helices (on the order of ten residues) could not form in aqueous solution.

The discovery of the C-peptide and S-peptide (Brown and Klee, 1971) forced a re-evaluation of the results of the host-guest experiments. These small peptides (13 and 20 residues, respectively) are formed during the cyanogen bromide cleavage of ribonuclease A. C-peptide consists of the first 13 residues of ribonuclease; S-peptide consists of the initial 20 residues of the protein. Both were substantially helical, a result that contradicted the conclusions of Scheraga's host-guest experiments. Baldwin and coworkers performed further experiments on these peptides, analyzing the interactions that stabilized the helical structure in detail (Kim and Baldwin, 1984; Shoemaker et al., 1985), and used the principles gleaned from these experiments to create other small peptides (Marqusee and Baldwin, 1987). An initial clue to an important source of helix stability was the observation that C-peptide lactone, formed during the cyanogen bromide cleavage of ribonuclease, had significant helicity, whereas cleavage of the lactone, regenerating the free carboxyl terminus of the peptide, abolished the helicity (Kim et al., 1982). This result was interpreted as confirming the hypothesis that interactions of formal charges with the macrodipole of the alpha helix could have a significant stabilizing effect (Shoemaker et al., 1985). Further work by Baldwin's group and others unearthed a wide range of stabilizing interactions in helical peptides: salt-bridges between side chains, in particular between residues in an  $i-i+4$  sequence register (Marqusee and Baldwin, 1987); manipulation of the charges on the amino and carboxyl terminus of the peptide to interact favorably with the helix dipole (Shoemaker et al., 1987); and aromatic and hydrophobic

interactions between side chains (Padmanabhan and Baldwin, 1994; Shoemaker et al., 1990). The inherent differences in the helix forming tendencies of the amino acids were also discovered to be much larger than Scheraga predicted. The strong helix forming propensities of some amino acids led to the *de novo* design of several peptides with large (~80%) helical content (Marqusee et al., 1989). This discrepancy has been attributed to the unsuitability of Scheraga's host systems for studying the properties of the guest residues; strong interactions between the side chains in at least one of the host systems masked the changes caused by the substituted guest residues (Padmanabhan et al., 1994). Studies by Kemp's group have tended to confirm some of Scheraga's results, but these results occur in a system incorporating a large organic molecule that serves as a helix initiator (Kemp et al., 1991), and may suffer from artifacts induced by the organic template molecule.

Chou and Fasman used a different method to study the relationship between primary and secondary structure. By surveying the frequency with which each amino acid appeared in a particular secondary structure, relative to the frequency with which that amino acid appeared in all proteins, they constructed a scale indicating the propensities of individual amino acids to appear in the context of the various secondary structures (Chou and Fasman, 1978). Chou and Fasman also studied the frequency of occurrence of amino acids at the ends of secondary structural elements. Thus amino acids which occurred often in an alpha-helical context became known as "helix formers", whereas a residue that often appeared at

the end of a helix was termed a "helix breaker." Similar values were compiled for beta sheets.

The work of Anfinsen, Chou and Fasman, and other researchers led to the hypothesis that "the folded conformation of a protein is thought to be dictated solely by its primary structure" (Creighton, 1993). Given the amino acid sequence of a protein, it should be possible, in theory, to predict the three-dimensional structure of the protein. In practice, substantial advances in computational capabilities and further analysis of sequences and structures would be required, but these were technical details to be overcome. Several groups made significant progress in relating primary to secondary structure, although these methods tended to hit a limit of around 65-70% accuracy (Rost et al., 1994).

However, there were also indications that this straightforward hypothesis--that a primary sequence dictated only one conformation--was an oversimplification; indeed, Anfinsen's original hypothesis had explicitly assumed a constant environment for the statement "sequence determines structure" (Anfinsen et al., 1961). Doty's experiments on amino acid polymers had shown that the same peptide could adopt different conformations, depending on the environment of the peptide and the method of preparing the solution. Polylysine, for example, adopted a random coil conformation in aqueous solution at pH 6.0 and 25°C (Rosenheck and Doty, 1961). At the same temperature, but at a pH of 10.8, polylysine adopted an alpha helical conformation. Heating the pH 10.8 solution to 52°C converted the peptide into a beta sheet conformation. By changing the solution conditions, the same

sequence (in this case, simply (Lys)<sub>n</sub>) could give rise to different structures. This was not completely unexpected, as it had long been known that heating proteins or adding compounds such as urea and guanidinium hydrochloride denatured proteins, changing their conformations from a folded state to a random coil state. The polylysine experiments, however, demonstrated a change from *one structured state to another* caused by the solution environment.

This uncertainty in relating sequence to structure was demonstrated in actual proteins (as opposed to the simple homopolymer models of Doty) when Kabsch and Sander studied the secondary structure of pentapeptides in proteins (Kabsch and Sander, 1984). They demonstrated that the identical pentapeptide sequence could be found in different structural states, for example in both beta sheet form and alpha helix forms, in different proteins. Cohen et al. (Cohen et al., 1993) extended this observation to hexapeptides and longer sequences.

Another example of ambiguity in assigning sequence to structure is seen in the beta sheet forming "KAK" peptides (Forood et al., 1995). These peptides are primarily composed of alanine and lysine, shown to be strong alpha helix forming residues in several independent studies (Bryson et al., 1995); one typical sequence is acetyl-K(A<sub>14</sub>)K-amide. Yet this peptide can be isolated in an extremely stable aggregated beta sheet conformation. This is remarkable considering that nearly identical peptides previously studied displayed high contents of alpha helix (Marqusee et al., 1989).

Clearly many factors besides the primary sequence influence the structure adopted by a polypeptide chain. The context of a protein in which a sequence is found, the pattern of residues appearing in the sequence, the solution conditions in which a sequence is studied, or even the method of preparation for study of a peptide sample, exert an effect on what conformation that sequence will adopt.

### **Switch Peptides**

The potential for structural ambiguity in a single sequence has been further confirmed by the study of "switch peptides," a term coined by Mutter to describe peptides which adopt different conformations under different conditions. Mutter's work in this area (Mutter et al., 1991; Mutter and Hersperger, 1990) focused on peptides which formed beta sheet structures in aqueous solution, but which adopted alpha helical states upon addition of trifluoroethanol (TFE), a strong helix inducing solvent. The most notable point of these studies was the rapid switch in structure over a relatively small change in the percentage of TFE added. Other researchers discovered peptides with the same rapid switch characteristic, and that the sharp change from beta sheet to alpha helix converted to a gradual increase when a single residue was replaced (Reed and Kinzel, 1993).

More recent work by Johnson (Waterhous and Johnson, 1994; Zhong and Johnson, 1992) examined the effect of solution additives

on peptide secondary structure. Peptides which were unstructured in aqueous buffer converted to alpha helical states when TFE was present in solution, and to beta sheet structure when non-micellar sodium dodecyl sulfate was present in solution. This further underscores the importance of considering the environment of a peptide or protein, as well as its sequence, in predicting the structure that the polypeptide will adopt.

Switch peptides have also been created by perturbing the chemical nature of side chains. Dado and Gellman (Dado and Gellman, 1993) created a "redox" switch peptide. In their peptide, methionine residues are strategically placed so that as reduced, nonpolar methionine, the peptide forms an amphiphilic alpha helix, but upon oxidation to polar methionine oxide, the peptide forms an amphiphilic beta sheet.

### **Azobenzene Switch Peptides**

An intriguing class of switch peptides utilize photochromic side chains to convert from one structure to another. The photoisomerizable compound azobenzene and its derivatives have been used extensively to create "photoswitch" peptides (Pieroni and Fissi, 1992); the photocleavable compound spiropyran has also been utilized in this manner (Pieroni et al., 1992). Azobenzene can be incorporated into peptides using the amino acid p-phenylazophenylalanine, in which an azobenzene unit is attached to the beta carbon of the amino acid (Goodman and Kossoy, 1966).



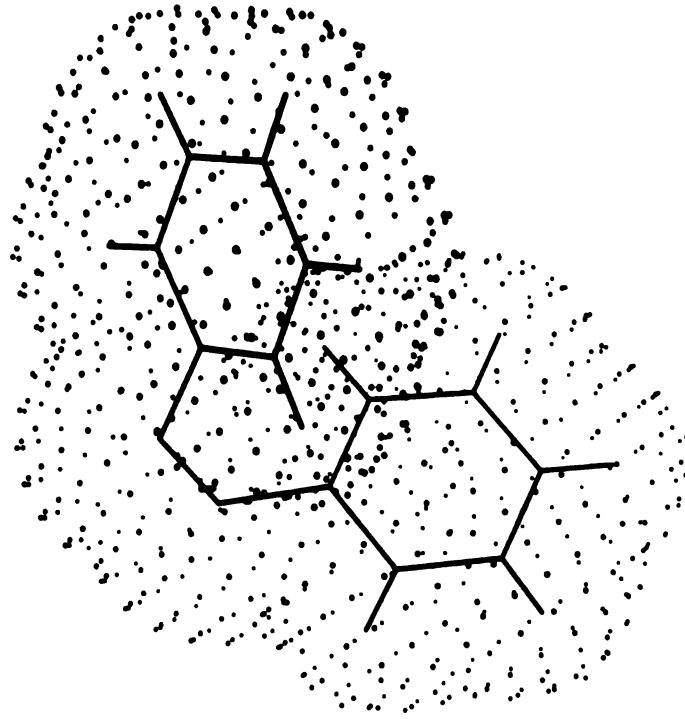
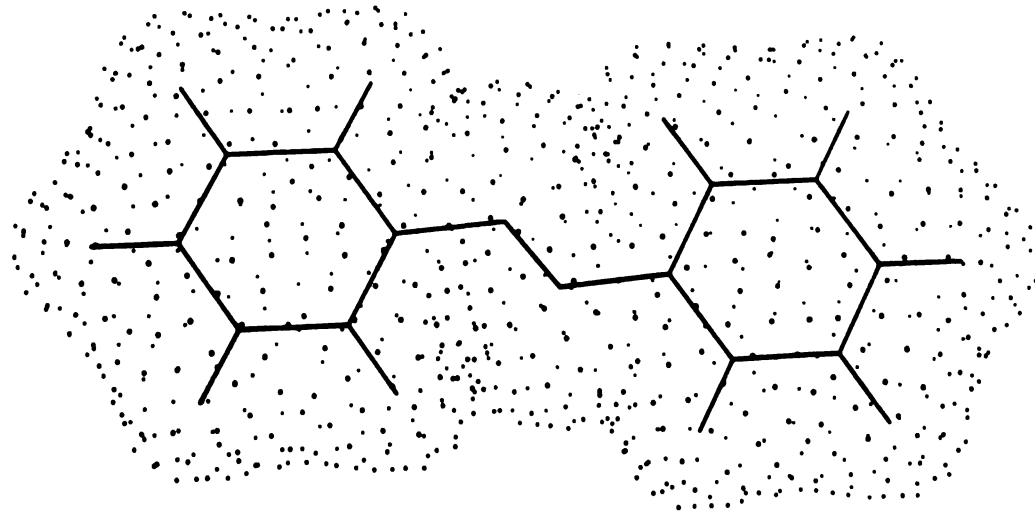


**Figure 1.** Trans (left structure) and cis forms of azobenzene.

Azobenzene derivatives may also be incorporated into peptides by attachment to natural residues, e.g. by coupling a carboxyl derivative of azobenzene to a lysine side chain or an amino derivative of azobenzene to an aspartate or glutamate side chain (Pieroni and Fissi, 1992). Azobenzene is particularly useful because of its stability to photodegradation and the reversibility of the *trans-cis* isomerization around the N-N double bond. Figure 1 shows the *trans* (Brown, 1966) and *cis* (Mostad and Rømming, 1971) states of azobenzene and their associated van der Waals surfaces. The essentially flat *trans*-azobenzene changes to a non-planar *cis* state upon photoisomerization; the obvious steric change is accompanied by a large change in the molecule's dipole moment, from approximately 0 Debye to about 3.0 Debye (Kumar and Neckers, 1989).

### **Biological Implications of Switch Peptides**

The dramatic changes in conformation displayed by switch peptides are not merely of theoretical interest. Research on several diseases, most notably Alzheimer's disease and prion diseases, has suggested that the pathology underlying the diseases is caused by a change in the conformation of peptides or proteins present in the organism. In the two aforementioned diseases, soluble, alpha helical forms of peptides and proteins are believed to convert to insoluble, beta sheet forms, precipitating out of solution in neuronal cells with disastrous consequences for the cell and the organism (Lansbury,

1995; Prusiner, 1994). Understanding why these conformational changes occur could aid efforts in controlling the diseases in humans.

There are many other biologically important processes that depend on conformational changes in proteins. The allosteric control of enzyme action is one of the oldest and most familiar. The strategy used by the influenza virus to gain entry to the cell from lysosomes, described in recent crystallographic studies, also depends on conformational changes to effect biological function. An important process driven by a photoisomerization event occurs in the rhodopsin molecule that enables vision: the retinal component of rhodopsin is isomerized by light, driving a conformational change in the protein component opsin, effecting subsequent changes in the cell enabling the cell to send a signal that light has been detected.

These processes and many others underscore the importance of conformational changes in peptides and proteins. It is possible that many factors are involved in a given process, and that different systems will rely on different combinations of forces. Having model systems to examine the importance of various factors in determining structure can help dissect the process of conformational change into its component parts, leading to a better understanding of important biological events.

## **Peptide Chemistry**

Many of the advances described in understanding the relationship of primary structure to secondary structure depend on

the ability of researchers to synthesize and characterize peptides of well-defined sequence and homogeneity. Peptides are of great interest in many other fields as well; many biological hormones and neurotransmitters are peptides; the immune system can be activated by peptides; several animal species, such as snakes and snails, use toxic peptides as defenses; and peptide pharmaceuticals are growing in importance as delivery and stability problems are resolved. Structural biology is one of only many fields that have taken advantage of the power of peptide chemistry and peptide synthesis.

Emil Fischer carried out some of the initial experiments in peptide synthesis at the beginning of the twentieth century. In addition to his pioneering scientific studies, Fischer also coined the terms "polypeptide" and "peptide". One of the most useful advancements in peptide synthesis was introduced in 1932 by Bergmann and Zervas: the benzyloxycarbonyl N-terminal protecting group, designated by the abbreviation Z in honor of Zervas. This group can be removed by the relatively gentle method of hydrogenolysis; by strong acids such as hydrogen bromide/acetic acid or hydrogen fluoride; or by Lewis acids such as trimethylsilyl iodide. The t-butyloxycarbonyl protecting group (abbreviated Boc) also proved to be useful in peptide synthesis due to its much greater acid lability (it can be removed by trifluoroacetic acid or by 4N HCl in dioxane). The coupling step in peptide synthesis, where two amino acids are condensed together to form a peptide bond, was also the focus of much effort. Acyl chlorides, acyl azides, anhydrides, carbodiimides, active esters, and phosphonium and uronium salts

provide the peptide chemist with a wide array of effective coupling techniques.

Even with the variety of alpha-amino and side-chain protecting groups and coupling reagents that had been developed, peptide chemistry in the 1950's was still quite a tedious business. A huge technological advance was provided by the work of R. Bruce Merrifield of the Rockefeller University. Merrifield's innovation consisted of utilizing an insoluble polymer support on which a single amino acid could be initially attached by reacting its carboxyl group with a functional group on the polymer support (typically polystyrene resin, on which a small percentage of the aromatic rings bore chloromethyl groups). The amino terminus of the amino acid would then be available for reaction. Adding another amino acid, with a protected amino group and activated carboxyl group, in an appropriate solvent, would elongate the amino acid on the resin to a dipeptide. The amino protecting group could be removed, and the cycle repeated by adding another protected, activated amino acid.

The great advantage of solid-phase peptide synthesis, as Merrifield's development was called, was that isolation of the intermediates in the synthesis was performed by the trivial step of removing the added reactants by separating the reaction solvent from the polystyrene resin on a filter; the growing peptide chain was retained on the resin ready for the next step in the synthesis. However, by-products such as peptide chains that were not elongated could no longer be separated after each step, leading to the build-up of side products on the resin. This problem was circumvented by using large excesses of coupling reagents and fine-

tuning the reaction conditions. With the introduction of improved coupling reagents, most notably the BOP reagent and its congeners and the HOAt reagent, and the development of optimal coupling conditions, coupling yields of 99.9% at each step are attainable, and peptides on the order of 100 residues have been synthesized successfully (Miller et al., 1989). The difficulty of separating the side products generated due to incomplete couplings remains the major barrier to synthesizing long peptides. Recently fragment coupling strategies have shown great promise in extending the length of peptides that can be synthesized chemically, and have made possible several interesting experiments in protein structure and chemistry. And advances in purification over the last three decades, particularly in high-pressure liquid chromatography (HPLC), have enabled isolation of synthetic peptides even in cases where significant synthetic by-products are present.

## **Circular Dichroism**

How does one go about the study of peptide and protein structure? Probably the majority of such studies begin with circular dichroism, a rapid method for overall structural assessment which requires relatively little sample and which is straightforward to perform. Circular dichroic (CD) spectroscopy relies on the differential absorption of left and right circularly polarized light by a chromophore in an asymmetric environment. The environmental asymmetry may be due to the structure of the chromophore itself, or

may arise by placing a symmetric chromophore in asymmetric surroundings. CD spectroscopy as applied to protein and peptide structure relies on the dichroism of the peptide bond--itself a symmetric chromophore--when placed in the chiral environment of an L-amino acid and structures formed by chains of L-amino acids (right-handed alpha helices, beta sheets, turns, and disordered structure). These structures give rise to characteristic spectra which can be theoretically predicted and examined experimentally (Woody, 1985). While the characteristic curves overlap to a great extent, methods for deconvoluting spectra and estimating the contribution of each type of secondary structure to a spectrum have been developed. These methods must be applied cautiously, but can yield useful information about the amount of each structural element present in a given sample (Johnson, 1990).

Circular dichroism can also be used to study time-dependent changes in secondary structure. Stopped-flow CD has shed light on protein folding events in the millisecond range (Elöve et al., 1992). Recent developments in time-resolved CD (and the related phenomenon of optical rotatory dispersion) hold promise for monitoring folding kinetics on nanosecond and picosecond time scales (Lewis et al., 1992).

CD has proven invaluable to the study of peptide secondary structure in solution. The relative ease of making CD measurements enables the spectroscopist to examine a wide range of solution conditions in a short period of time. However, artifacts can arise in a variety of situations, which complicates the interpretation of results; resolution of these complications may require the use of other types

of experiments to corroborate the CD results. CD measurements are generally made in the far UV region for peptide secondary structure (roughly 190-230nm, corresponding to the  $n-\pi^*$  and  $\pi-\pi^*$  electronic absorption bands of the amide bond). Any other chromophores which absorb in these regions and which are in a chiral environment may also have a CD signal, interfering with the signal arising from the peptide bonds. In particular, tyrosine and tryptophan have the potential to distort CD spectra of peptides and proteins (Chakrabarty et al., 1993c). Other possible distortions may arise when the secondary structure of the system under study deviates slightly from the "typical" secondary structures of the reference systems used to establish the characteristic CD curves (e.g., CD signals arising from a kinked alpha helix may differ from those arising from a perfectly straight helix) (Manning et al., 1988).

Circular dichroism is ultimately limited in the amount of information it can provide. Because it assesses the environment of all amide bonds simultaneously, CD only gives a global assessment of the secondary structure present in a peptide, not a residue-by-residue report. Furthermore, a CD spectrum indicating 50% alpha helix and 50% random coil could arise from very distinct samples: a sample where all peptides have half of their residues in an alpha helical conformation and half in random coil conformation, and a sample where half the peptides have all of their residues in an alpha helical conformation and half have all residues in random coil conformation.

Despite its limitations, circular dichroic spectroscopy is a useful and rapid method for studying secondary structure; when used



properly, it is a powerful technique in the repertoire of the structural biophysicist.

## **Infrared Spectroscopy**

Infrared absorption spectroscopy has developed into another useful tool for the determination of secondary structure in peptides and proteins. Shifts in the IR absorption frequencies of the amide bond, caused by the differences in the hydrogen bonding patterns between the various types of secondary structure, provide means for determining the secondary structures present in the polypeptide. The most useful band for structure determination is the amide I band (if the amide carries a deuterium in place of the hydrogen, the band is designated I'), which appears in the region from 1600 to 1700  $\text{cm}^{-1}$ . Instruments operating in the Fourier transform mode (FTIR) have almost completely displaced continuous-sweep IR as the method of choice.

As in CD spectroscopy, artifacts can be introduced by chromophores absorbing in the amide I region; the side chains of glutamine, asparagine, and to a minor extent tyrosine interfere with the IR measurement. IR spectroscopy also tends to rely much more heavily than CD does on mathematical processing after spectral acquisition, to resolve highly overlapped bands when more than one secondary structure is present. This presents another opportunity for the introduction of artifacts into the spectra and subsequent misinterpretation.

A useful feature of FTIR involves introduction of isotopic labels (e.g.,  $^{13}\text{C}$ ) at one or more locations in the peptide chain. This can shift the absorption band of particular residues into an uncrowded region of the spectrum, allowing residue-specific determination of secondary structure in a peptide. Because this requires a special synthesis of labelled peptide, however, it is of use mainly in small systems or peptides where the environment of a certain residue is of particular importance.

FTIR spectroscopy provides a satisfactory alternative to CD spectroscopy for secondary structure determination in peptides and proteins. Given the distinct physical bases for the two methods, they complement each other well. In particular, artifactual problems that arise in one type of spectroscopy may be absent in the other type. Recent studies utilizing both methods for structural determination indicate that the two methods together are more reliable than either one used separately. When possible, the peptides studied in this thesis have been examined using both CD and FTIR spectroscopies.

## **Nuclear Magnetic Resonance**

The most powerful technique available for conformational analysis of peptides in solution is multidimensional nuclear magnetic resonance (NMR). NMR rapidly advanced from its origins in studying nuclear spin to become the most widespread experiment for analyzing solution structures of macromolecules at atomic level resolution. The number of NMR experiments available for analyzing structure has grown explosively in recent years, and advances in

instrumentation, computational resources, and mathematical methods have also contributed greatly to the growth in NMR. The multidimensional nuclear Overhauser effect experiment (NOESY) offers a wealth of information on peptide structure on a residue-by-residue basis. Because of the high cost of introducing isotopic labels into synthetic peptides, NMR studies on peptides primarily utilize homonuclear experiments.

Nuclear magnetic resonance studies of peptide secondary structure are far less prone to artifacts than either CD or FTIR experiments. While artifacts can certainly arise during the collection and processing of NMR data, these problems generally interfere with the quantitative interpretation of experiments rather than the qualitative interpretation. The necessity for relatively large amounts of sample (approximately 400 microliters) and high concentrations (between one and ten millimolar) is one of the few disadvantages of NMR relative to CD and FTIR. Aggregated molecular assemblies, such as multimeric beta sheets, tend to be difficult to study by solution NMR for various reasons; this is another circumstance where CD and IR studies can provide information which is difficult to obtain by NMR.

### **Design of Peptides Used in This Study**

The peptides described in this study are derived from a family of peptides originally designed to serve as test systems for alpha

helical behavior (Bradley et al., 1990). The sequences of these peptides are shown in Figure 2.

**PEPTIDE I:**

**acetyl-ETATKAELLAKYEATHK-amide**

**PEPTIDE II:**

**acetyl-ETATKAELLAKZEATHK-amide**

**Figure 2. Sequences of peptides used in this study. Z= p-phenylazo-L-phenylalanine.**

Several factors were taken into account to ensure the helicity of the designed peptides. Residues with negatively charged side chains were placed towards the N-terminus, and residues with positively charged side chains were placed towards the C-terminus. This positioning causes a favorable interaction with the helix macrodipole, thus lowering the energy of a helical state relative to a random coil state. Residues were also aligned to create *i, i+4* spaced salt bridges in the helical state between glutamate and lysine side chains, and the salt bridges were also aligned so as to interact favorably with the helix dipole moment. Most of the residues--glutamic acid, lysine, alanine, and leucine--are good helix formers according to Chou-Fasman criteria. Other residues--threonine, glycine, histidine, and tyrosine--were also included. These residues facilitate structural characterization by NMR, by varying the amino

acid composition. Tyrosine provides a convenient absorption band with which to measure peptide concentration by UV absorption. The overall amino acid content was chosen with the need for high water solubility in mind; hence the high number of charged residues. The potential for aggregation of helices was minimized by avoiding amphiphilicity in the helical state, which would create a hydrophobic face favoring dimerization (for an example of a peptide designed with dimerization in mind, see (Schafmeister et al., 1993)).

While these design principles successfully enabled formation of an alpha helix, a second design was (inadvertently) built into the peptide that favored beta sheet, not alpha helix, formation. Figure 3 illustrates how the peptide could form an amphiphilic beta sheet, with stabilizing salt bridges between adjacent strands. This is a familiar design principle, which has been exploited by other researchers (Brack and Spach, 1981; Osterman and Kaiser, 1985), albeit not in the context of switch peptides. Figures 4 and 5 show peptide I in sheet and helix conformations, respectively (these are model structures generated by using standard phi, psi angles).

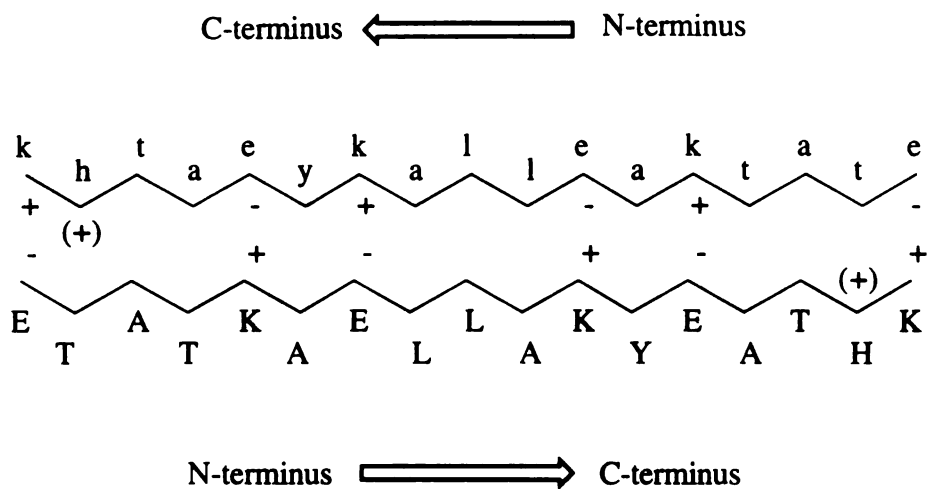
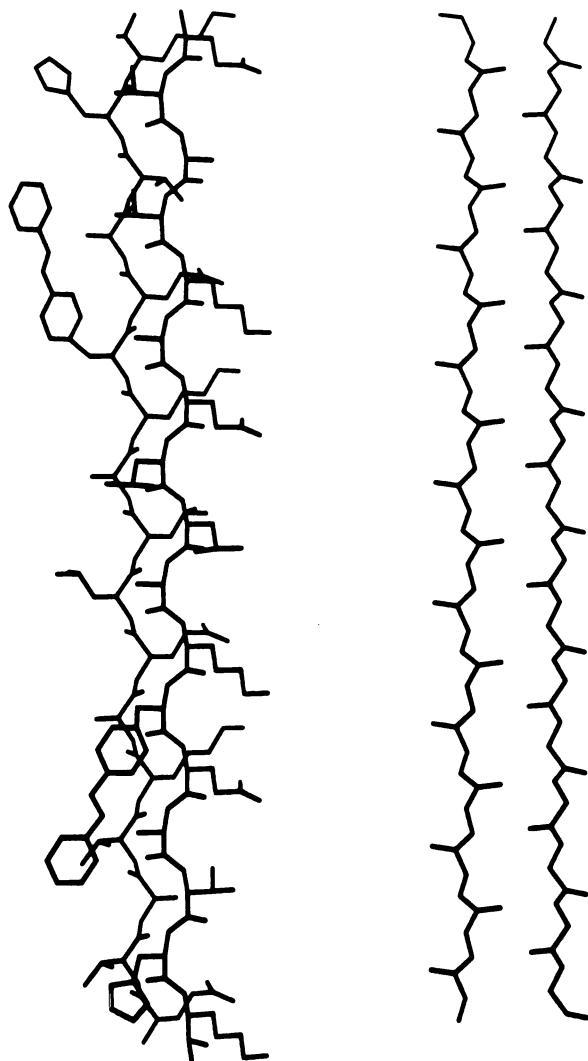
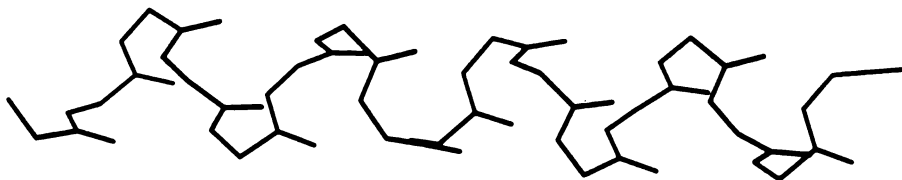
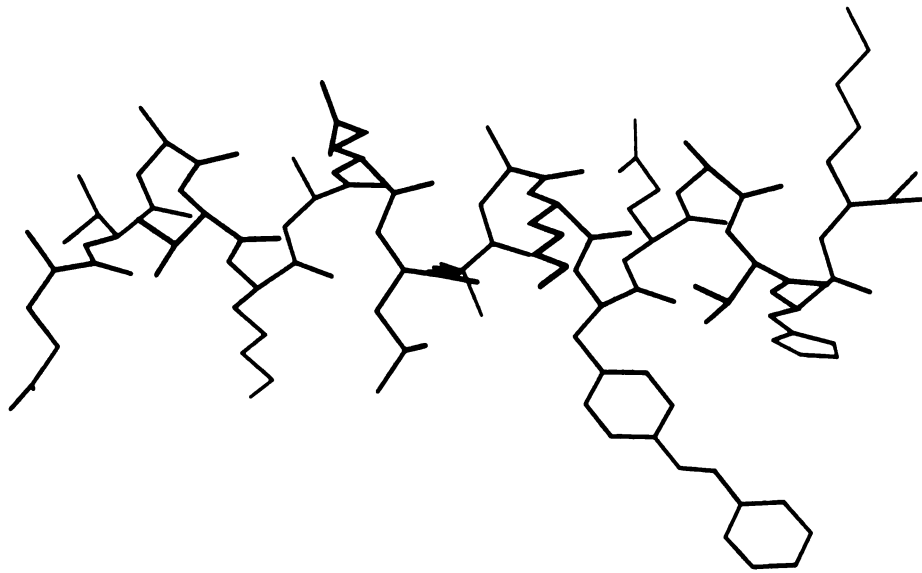


**Figure 3. Peptide in antiparallel beta-sheet conformation.** Only two strands are shown for clarity; additional strands can aggregate on either edge and propagate the structure indefinitely. Residues that may be charged are indicated by + or -.



UCSF MidasPlus

**Figure 4.** Peptide II in a model antiparallel beta sheet conformation. Only two strands are shown for clarity; an indefinite number of strands may aggregate. The left figure shows side chains in an extended conformation; the right figure shows only mainchain atoms.



UCSF MidasPlus

**Figure 5.** Peptide II in a model helix conformation. The top figure shows side chains in an extended conformation; the bottom figure shows only mainchain atoms.



Given the potential to form two extremely different ordered structures, alpha helix and beta sheet, what determines which structure the peptide will adopt? By examining the two models of secondary structure, some tentative predictions can be made. Because the alpha helix is a monomeric structure, whereas the beta sheet is a multimeric structure, the concentration of peptide in solution should affect the structure adopted; dilute solutions would favor a monomeric, helical state, while concentrated solutions should favor a beta sheet aggregate. The pH dependence of the charges on the side chains would yield a net charge of +4 at low pH, discouraging aggregation (and favoring helix), whereas at neutral pH the peptide would have a net charge of zero and aggregation would not need to overcome charge repulsion between monomers.

In this study, several factors were explored to examine their effect on the structural preference of the peptides. Various peptide concentrations, pH values, salt concentrations, and temperatures were explored.

An additional factor involved in the design of one peptide was the incorporation of the artificial residue, p-phenylazo-L-phenylalanine (Goodman and Kossoy, 1966), effectively adding an azobenzene group as a side chain at position 12. The photoisomerizable side chain of the phenylazophenylalanine residue provides yet another variable affecting the balance between alpha helix and beta sheet. As described above, in the *trans* state of azobenzene, which tends to be the most stable conformation, the rings lie in a plane and the molecule has a very small dipole moment. The *cis* state, however, is nonplanar and has a large dipole moment.

This dramatic difference in steric and electronic characteristics of the side chain has the potential to affect the overall conformational preference of the peptide, as has been demonstrated in several other peptide systems (Pieroni and Fissi, 1992). Because of the interactions between the tyrosine at position 12 and the histidine at position 16 in the parent peptide (Bradley et al., 1990), the tyrosine was replaced with phenylazophenylalanine in anticipation of a significant perturbation upon photoisomerization of the side chain. One application of a peptide capable of conformational changes when irradiated would be monitoring the folding or unfolding kinetics of secondary structure; rapid spectroscopic techniques have been developed which can detect such changes on nanosecond and picosecond time scales.

The original goal of the work presented here was to create a system with which to study the kinetics of the alpha helix-random coil transition. The incorporation of p-phenylazophenylalanine was made with the expectation of producing a perturbation in the *helical* state of the peptide. However, the tyrosine-phenylazophenylalanine mutation enabled the peptide to adopt beta sheet conformations, in addition to its helical states, as monitored by CD and FTIR. The conditions under which this occurs, and the underlying forces that influence which folded state the peptides adopt, are the subject of this thesis. A manuscript submitted for publication forms the appendix, and covers the main points of the thesis in a more concise fashion.

## EXPERIMENTAL

### Synthesis of Fmoc-p-phenylazo-L-phenylalanine

Fmoc chemistry was chosen because of the relatively mild coupling and cleavage conditions. No previous solid phase peptide syntheses using azobenzene-containing residues could be found in the literature, but studies of azobenzene-containing peptides had been performed in the solvent trifluoroacetic acid (TFA), which is used during Fmoc peptide cleavage procedures. This known stability of azobenzene in TFA, combined with the unknown stability of azobenzene during the hydrogen fluoride cleavage procedures of Boc chemistry, made Fmoc chemistry the preferred method for peptide synthesis.

The procedure of Goodman and Kossoy (Goodman and Kossoy, 1966) was used to synthesize p-phenylazo-L-phenylalanine. 3.0 g (14.4 mmole) of p-amino-L-phenylalanine (Sigma) was placed in a round bottom flask equipped with a magnetic stirbar and dissolved in 30 ml acetic acid. 1.55 g (14.4 mmole) of nitrosobenzene (Aldrich) was added in small solid portions to the solution over a period of 40 minutes. The solution was pale yellow prior to addition of nitrosobenzene; addition of the nitroso compound caused the solution to turn dark brown. The reaction was allowed to proceed for another 15 minutes; fine orange precipitate was visible. 200 ml of distilled water was added, causing large clumps of precipitate to fall out of solution. The solution was placed in the refrigerator overnight; then

the precipitate was filtered off on a fritted funnel and washed with distilled water, ether, and hexane. After drying under vacuum with P<sub>2</sub>O<sub>5</sub>, the orange-brown precipitate weighed 1.46 g; the yield of crude p-phenylazo-L-phenylalanine was 5.4 mmole (38%).

The Fmoc derivative used for solid phase synthesis was synthesized using fluorenylmethylsuccinimidyl carbonate (Atherton and Sheppard, 1989). 0.53 g sodium carbonate (5.0 mmole) was dissolved in 20 ml distilled H<sub>2</sub>O. 1.03 g (3.8 mmole) of the crude p-phenylazo-L-phenylalanine product was added. 40 ml of acetone, 20 ml of distilled water, and portions of sodium carbonate were then added, and the solution filtered through a sintered glass funnel to remove insoluble particles. The solution was dark orange. 1.23 g (3.65 mmole) fluorenylmethylsuccinimidyl carbonate (Aldrich) was dissolved in 20 ml acetone and added in portions over a period of 55 minutes. The pH of the solution was maintained between 8 and 9 by periodic addition of more sodium carbonate. Precipitate was observed approximately 1 hour after addition of fluorenylmethylsuccinimidyl carbonate was finished; 7 hours after addition was finished, the reaction was terminated by the addition of 1 N HCl until the pH was between 1 and 2. Large amounts of precipitation occurred during acidification. The precipitate was filtered off, washed with 1 N HCl and hexane, and dried under vacuum overnight. The crude Fmoc-p-phenylazo-L-phenylalanine weighed 1.63 g (3.3 mmole, 87% yield). HPLC analysis (on a Vydac C4 analytical column, run under isocratic conditions of 50% water/50% acetonitrile containing 0.1% TFA) of the crude material showed a main peak accounting for approximately 72% of the

absorbance when monitored at 215 nm and 98% of the absorbance when monitored at 325 nm. Fast atom bombardment (FAB) mass spectral analysis showed a major peak at 492.1 mass units, corresponding to the expected  $MH^+$  peak of Fmoc-phenylazophenylalanine, and another peak at 583.1 mass units. Numerous attempts at recrystallizing or otherwise purifying the Fmoc-phenylazophenylalanine did not succeed in improving the purity significantly, so peptide II was synthesized using the crude material. Mass spectral data showed no sign of any +91 mass unit component after peptide II purification (see below), so proceeding with the crude amino acid was not problematic.

Subsequent to the two-step synthesis of Fmoc-phenylazo-L-phenylalanine, a direct, one-step synthesis was developed that resulted in a much cleaner product. This synthesis utilized Fmoc-p-amino-L-phenylalanine as a starting material. 3.0 g (7.4 mmole) of Fmoc-p-amino-L-phenylalanine (Bachem) was placed in a 500 ml round bottom flask equipped with magnetic stirring. 250 ml of acetic acid and 65 minutes of vigorous stirring were necessary to dissolve the protected amino acid completely; it formed a pale yellow solution. 793 mg (7.4 mmole) of solid nitrosobenzene was added in small portions over 65 minutes. Starting material could still be detected by thin-layer chromatography 5 hours after the addition of nitrosobenzene was completed; some precipitate was also visible. The reaction was stopped at this point by the addition of 225 ml of distilled water, which caused massive precipitation of orange-brown material to occur. The reaction solution was stored at 5°C overnight; still more precipitate was visible the following morning. Purification

was accomplished by dissolving 0.5 g crude Fmoc-p-phenylazo-L-phenylalanine in 225 ml of ethyl acetate (heating on a steam bath was necessary for complete dissolution), extracting with four portions of 100 ml distilled water, then with four portions of 0.024 N HCl solution. The ethyl acetate layer was evaporated and the amino acid redissolved in acetone. The amino acid was recrystallized from an acetone/0.024 N HCl solution. HPLC analysis of this material showed it to be greater than 98% pure when analyzed by C4 reverse phase HPLC with detection at 215 nm (isocratic elution, 50% H<sub>2</sub>O/50% acetonitrile, containing 0.1% TFA). The amino acid was dissolved in the isocratic running buffer (50% H<sub>2</sub>O/50% acetonitrile, with 0.1% TFA) for injection; it was observed that a second peak appeared in the analysis if the sample was not immediately injected onto the column.

## **Peptide Synthesis**

Peptides were synthesized on an Applied Biosystems, Inc. (ABI) Model 431A peptide synthesizer using Fmoc (9-fluorenylmethoxycarbonyl) chemistry. Benzotriazolyl tetramethyluronium hexafluorophosphate (HBTU)/hydroxybenzotriazole (HOBt) coupling reagents were used for peptide I; dicyclohexylcarbodiimide/HOBt coupling reagents were used for peptide II. Standard Fmoc amino acids were purchased from Millipore; reagents were purchased from ABI and Aldrich, and solvents from ABI or Baxter. Double coupling of standard Fmoc

amino acid residues was employed. The following ABI protocol ("standard scale Fmoc") was used for synthesis:

DEPROTECTION	1X 3 minute wash, 20% piperidine in NMP
	1X 20 minute deprotection, 20% piperidine in NMP
WASHES	6X resin washed with NMP
COUPLING	71 minutes of coupling with 1 mmole of activated amino acid
WASHES	7X resin washed with NMP
SECOND COUPLING	71 minutes of coupling with 1 mmole of activated amino acid
WASHES	7X resin washed with NMP

The ABI Fmoc coupling protocol calls for a fourfold excess of activated amino acid to resin-bound peptide (1 mmole of activated amino acid is used to couple to 0.25 mmole of resin-bound amine). To conserve phenylazophenylalanine, for the incorporation of that amino acid into the peptide only two equivalents and a single coupling were used, over a coupling period of 2 hours (the standard

ABI coupling period for Fmoc chemistry is 71 minutes). A qualitative Kaiser ninhydrin test was essentially negative, indicating that coupling was substantially complete. The standard ABI protocol was resumed afterwards for the completion of the peptide. Millipore PAL resin was used to generate carboxy-terminal amide groups, and the amino terminus was acetylated.

Peptide I was cleaved using 95% trifluoroacetic acid/3% anisole/1% ethanedithiol/1% thioanisole. After 90 minutes, the solution was filtered, the volume reduced by evaporation, and the peptide was precipitated by adding cold ether. The precipitate was redissolved in distilled H<sub>2</sub>O, and lyophilized. Peptide II was cleaved with 80% trifluoroacetic acid/8% anisole/4% ethanedithiol/4% thioanisole. As peptide II tended to form an oil upon addition of ether to the TFA solution, the cleavage solution was evaporated and the excess scavengers separated from the colored peptide oil by pipette. The oil was then redissolved in distilled H<sub>2</sub>O and lyophilized.

The crude peptides were purified by reverse-phase HPLC on Vydac C-18 semipreparative columns using a water/acetonitrile gradient containing 0.1% TFA, monitoring elution at either 275 nm (peptide I) or 325 nm (peptide II). Peptide I was subjected to a second purification on a Vydac C-4 semipreparative column using water/acetonitrile/TFA solvents. The identity of the purified peptides was established by FAB mass spectrometry (peptide I, MH<sup>+</sup> 1945.3 calc., 1945.1 found; peptide II, MH<sup>+</sup> 2033.1 calc., 2033.3 found); the mass spectra are shown in Figures 6 and 7. No peptide



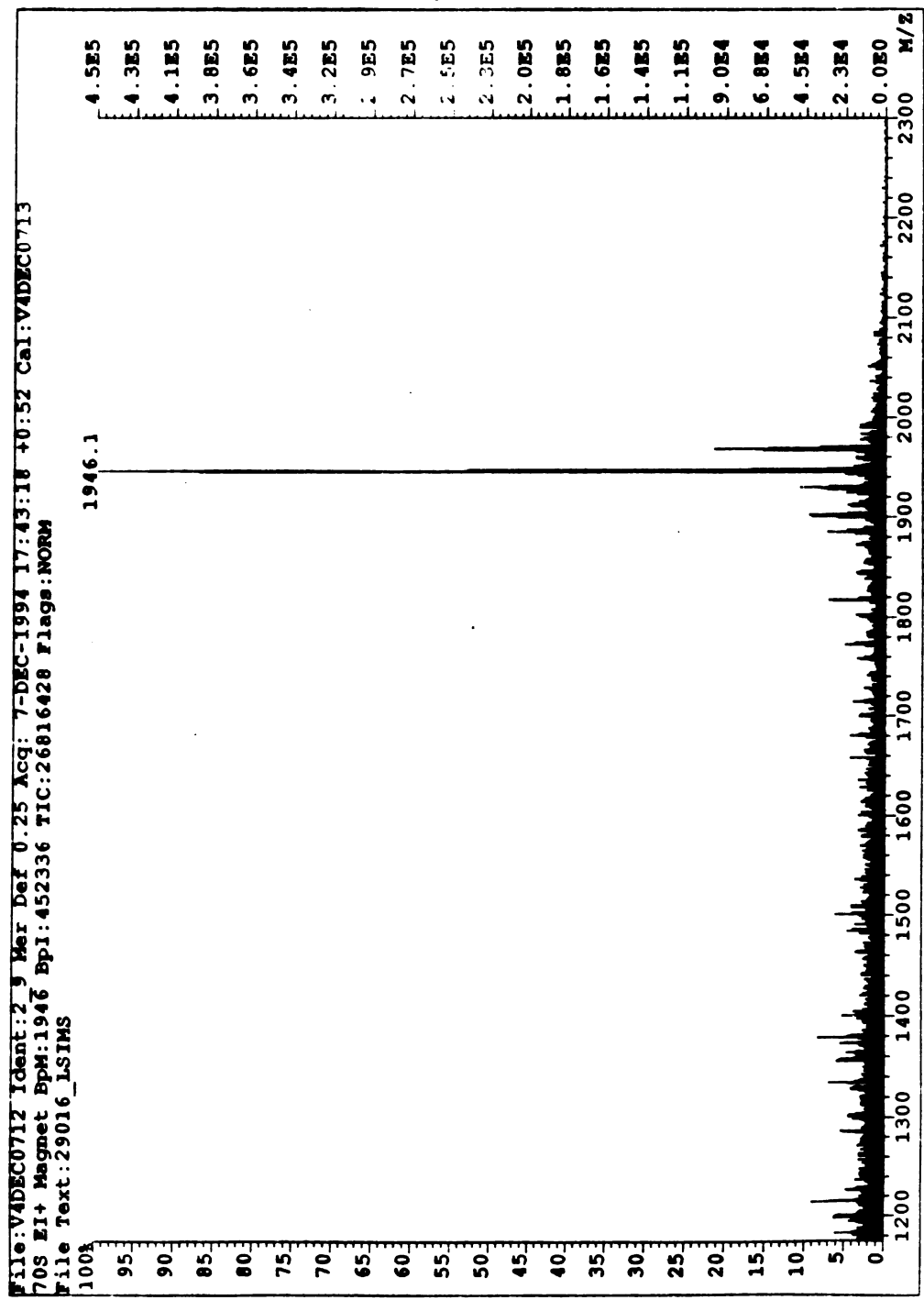


Figure 6. Mass spectrum of purified peptide I.



product at higher mass was found for peptide II, indicating that the contaminant in the artificial amino acid described in the previous section was either not incorporated into the peptide or that peptides containing the undesired side product were successfully removed during purification. (For both peptide I and II, the sodium adduct was also observed in the FAB mass spectra).

Peptide purity was assayed by HPLC on a Vydac C-18 analytical column, with detection at 215 nm. The initial purity of peptide I was 94% pure; peptide II was initially 99% pure and consisted of an 8:1 mixture of *trans:cis* isomers of the phenylazophenylalanine side chain (the peak consisting of pure *trans* isomer was isomerized on passage through the HPLC UV detector). HPLC traces of the purified peptides are shown in Figures 8 and 9. For the studies in this thesis, the peptides were generally recycled afterwards for further experiments by another round of HPLC, so the purity of the peptides was maintained or improved over the initial level with each set of experiments.

### **Circular Dichroism**

Circular dichroism measurements of peptide II were made on a Jasco J-500 spectropolarimeter. Circular CD cuvettes of varying pathlengths were used; temperature control was maintained by means of a jacketing cell holder through which a thermostatted water bath passed. Temperature was monitored by use of a thin-wire thermocouple which could be placed directly in the sample. A

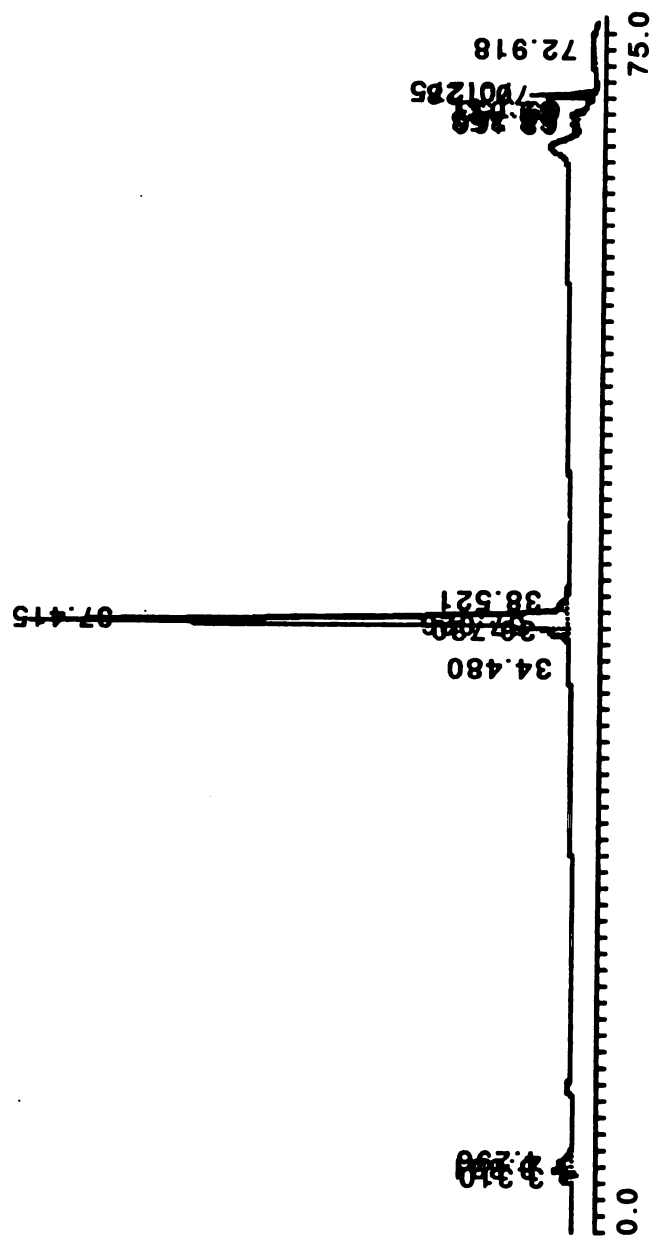


**Figure 8.** HPLC trace of purified peptide I. The region integrated for purity calculation excluded the early injection spike and late wash artifacts.

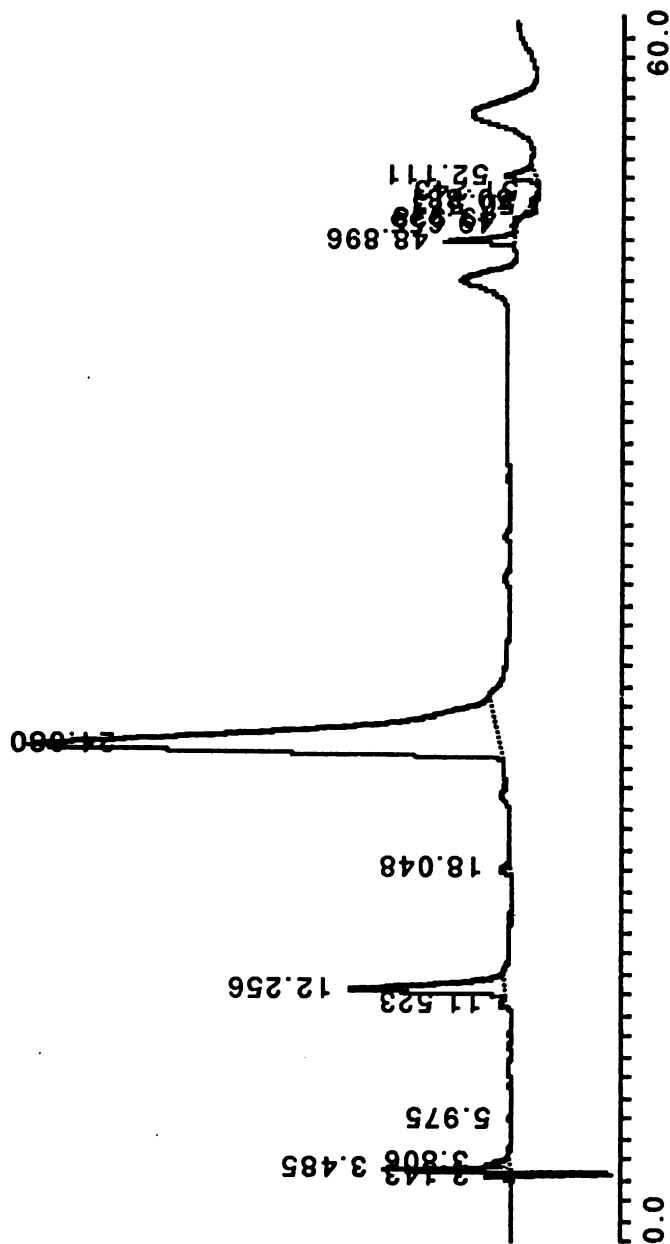


**Figure 9.** HPLC trace of purified peptide II. The region integrated for purity calculation excluded the early injection spike and late wash artifacts.

baseline spectrum, acquired under identical conditions as the sample spectrum, was subtracted from the sample spectrum unless otherwise indicated. In general, the baselines recorded for the circular cells were flat, and simply corrected for a constant offset of the spectra from zero.

CD measurements on peptide I were carried out on a Jasco J-710 spectropolarimeter. Rectangular cells of varying pathlength were used. Temperature control was achieved by placing the cell inside a closed Peltier control unit. All spectra were corrected by subtracting a baseline spectrum from the sample spectrum. Unlike the flat baseline spectra recorded for the circular cells, the baselines for the rectangular cells were irregular. This is due to the increased amount of window strain in rectangular cells as compared to circular cells (Johnson, 1985). Even after baseline correction, the region near 260 nm, while flat, was often offset from zero. This region was set to zero by subtracting the average of the data from 256 nm to 260 nm.

No smoothing was performed on any of the spectra presented. Spectra taken on the Jasco J-500 machine, an older instrument, typically had significant amounts of noise present. No important features of the spectra were obscured, however. Spectra obtained on the Jasco J-710, a newer and improved spectrometer, typically had little observable noise, even after a single scan.

## **Fourier-Transform Infrared Spectroscopy**

IR spectra were acquired on a Perkin-Elmer System 2000 FTIR microscope. A 50  $\mu\text{m}$  pathlength cell with calcium fluoride windows was used. The HPLC-purified peptides were lyophilized at least twice out of 20 mM HCl solution to remove traces of TFA (which has a band in the amide I region important in peptide structure determination), then lyophilized once from D<sub>2</sub>O solution. The dry deuterated peptides were then taken up in D<sub>2</sub>O buffers immediately before acquiring spectra. The pH\* of solutions was measured after acquiring spectra, to avoid introducing H<sub>2</sub>O prior to experiments, and are reported here uncorrected. The generally accepted equation for correction of pH due to isotope effects is  $\text{pD} = \text{pH}^* + 0.4$  (Glasoe and Long, 1960).

Spectra of the buffers were also acquired under identical conditions and subtracted from the peptide spectra. Because of the near-impossibility of exactly matching the water vapor content of the IR microscope chamber during two separate runs, a substantial amount of water vapor signal remains even after buffer subtraction. To correct for this on peptide II, the sharp water peaks were removed by linear interpolation between "true signal" points. This invariably requires subjective interpretation of where the water peaks begin and end on the underlying broad peptide peaks. Fortunately the difference in linewidths (a few  $\text{cm}^{-1}$  for water peaks versus approximately 20  $\text{cm}^{-1}$  for peptide peaks) is sufficient for this purpose, as the sharp water peaks are easily distinguishable from the broad peptide peaks. To correct for residual water signal on peptide I, a spectrum was taken of an empty IR cell, with neither sample nor buffer in the beam path. This provided a spectrum of

water vapor in the IR microscope chamber. This spectrum was subtracted from the sample spectrum *after* the buffer spectrum had been subtracted from the sample spectrum. With appropriate scaling of relative intensities, it was possible to eliminate most of the H<sub>2</sub>O vapor signal from the final spectrum.

The spectrum in Figure 20 was smoothed by converting it into its corresponding frequency components, and then attenuating the higher frequencies. The attenuation algorithm removed components in a certain range completely (typically the highest 20% of the frequencies) and then linearly increased the contribution of the remaining frequencies, with the lower frequencies having the greatest weighting. The spectra in Figure 21 were smoothed by averaging each data point with neighboring data points.

In most spectra presented here, the amide I' region was fitted to a flat baseline. No self-deconvolution was used, as the interconversion of bands corresponding to alpha helix and beta sheet was apparent from simple inspection of spectra.

## **Ultraviolet Irradiation**

Peptide II solution (75 uM peptide) was placed in a glass cell and the cell was placed in a Pyrex beaker containing water and ice (replenished periodically) to prevent heating of the sample. The beaker was then placed a few inches from a medium pressure Hanovia L679A 450 W lamp (equipped with a Pyrex glass shield to remove short-wavelength light) for 60 minutes. CD spectra were then acquired within 10 minutes after ending irradiation.



## **Nuclear Magnetic Resonance Spectroscopy**

NOESY, COSY, and HOHAHA spectra of peptide I in 90% H<sub>2</sub>O/10% D<sub>2</sub>O at 15°C, 5 mM peptide concentration, pH 2.4, were recorded on a General Electric 500 MHz Omega system, using presaturation to suppress the water signal. Four NOESY spectra of peptide I were co-added to generate a single spectrum with 64 acquisitions per t<sub>1</sub> increment; COSY and HOHAHA spectra were recorded with 16 acquisitions per t<sub>1</sub> increment. A NOESY spectrum of peptide II in 90% H<sub>2</sub>O/10% D<sub>2</sub>O was recorded on a Varian Unity 600 MHz spectrometer at 15°C, 460 μM peptide concentration, pH 2.4, using a 10 mm probe; 16 acquisitions per t<sub>1</sub> increment were recorded and symmetrically-shifted pulses were used for water suppression (Smallcombe, 1993). A mixing time of 150 msec was used for both peptide I and II NOESY spectra. All spectra were acquired with 2K complex points in the t<sub>2</sub> dimension and 512 complex points in the t<sub>1</sub> dimension. They were zero-filled once and apodized with a sin<sup>2</sup>70 function. The spectra were processed using the Striker software and baseline correction software developed at UCSF by Mark Day (unpublished). The spectra were inspected and assigned using the Sparky software developed at UCSF by Don Kneller (unpublished).

## RESULTS

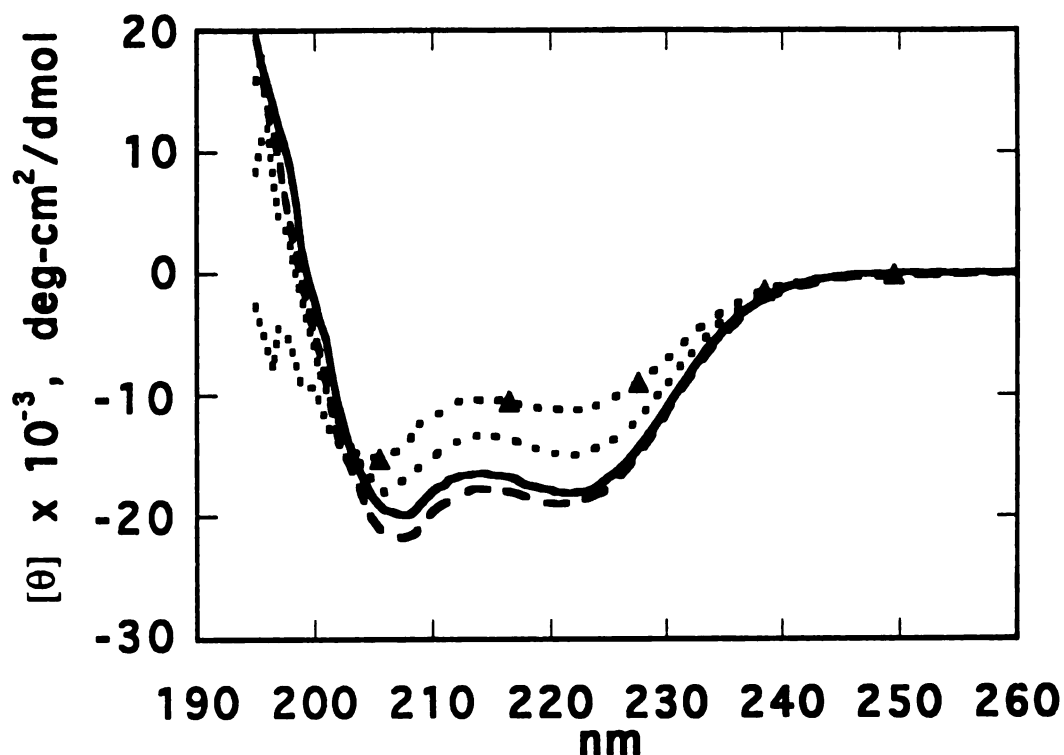


**Figure 10. Peptide I pH titration, 100  $\mu\text{M}$  peptide concentration.** pH 2 (—); pH 4 (---); pH 6 (·····); pH 8 (-·-▲-·-). Spectra taken at 5°C. 100 mM NaCl/1 mM Na citrate/1 mM Na phosphate/1 mM Na borate buffer.

*pH titration.* Circular dichroism spectra of the pH titration of peptide I, at 100  $\mu\text{M}$  peptide concentration, are shown in Figure 10; the mean residue ellipticity at 222 nm is plotted versus pH in Figure 11. The buffer solution contains 100 mM NaCl and 1 mM each of sodium citrate, phosphate, and borate. The peptide spectra are typical of partially helical peptides, displaying two minima at approximately 222 nm and 205-208 nm with an isosbestic point at

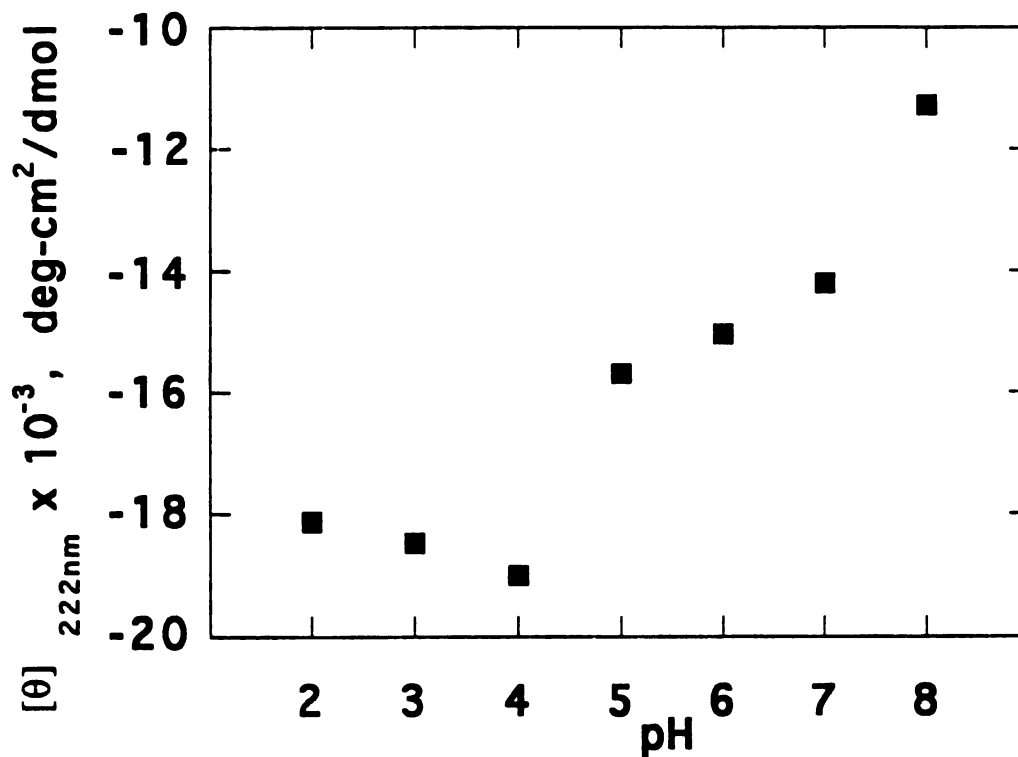


**Figure 11. Peptide I pH titration, 100  $\mu$ M peptide concentration.** Mean residue ellipticity  $[\theta]$  at 222 nm from pH 2 to pH 8. Spectra taken at 5°C. 100 mM NaCl/1 mM Na citrate/1 mM Na phosphate/1 mM Na borate buffer.

203 nm. The helical structure increases slightly from pH 2 to 4, and then drops rapidly from pH 4 to 5, continuing to decrease as the pH increases.

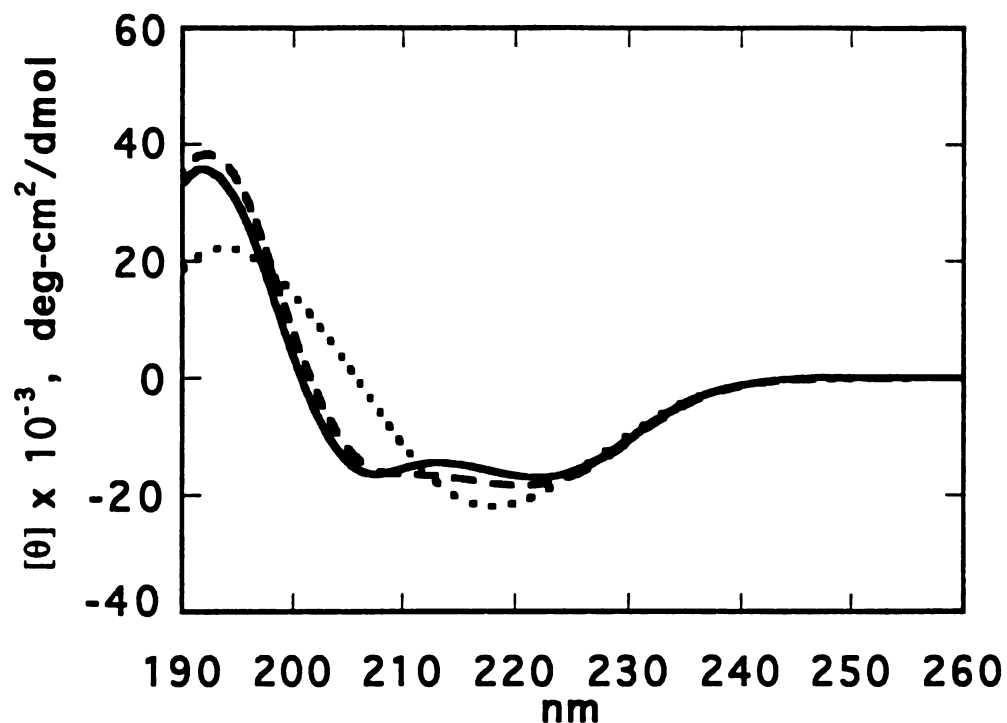


**Figure 12. Peptide I pH titration, 1.2 mM peptide concentration.** pH 2 (—); pH 4 (---); pH 5 (·····). Spectra taken at 5°C. 100 mM NaCl/1 mM Na citrate/1 mM Na phosphate/1 mM Na borate buffer.

Increasing the peptide I concentration to 1.2 mM results in much different behavior over the pH titration range. The peptide displays helical spectra at pH 2 (Figure 12) and 3 (not shown). At pH 4, the curve is starting to distort somewhat, but is still recognizably alpha helical. However, at pH 5, the spectrum is most suggestive of beta sheet structure (a single minimum at 218 nm) and the peptide solution was cloudy (Figure 12).

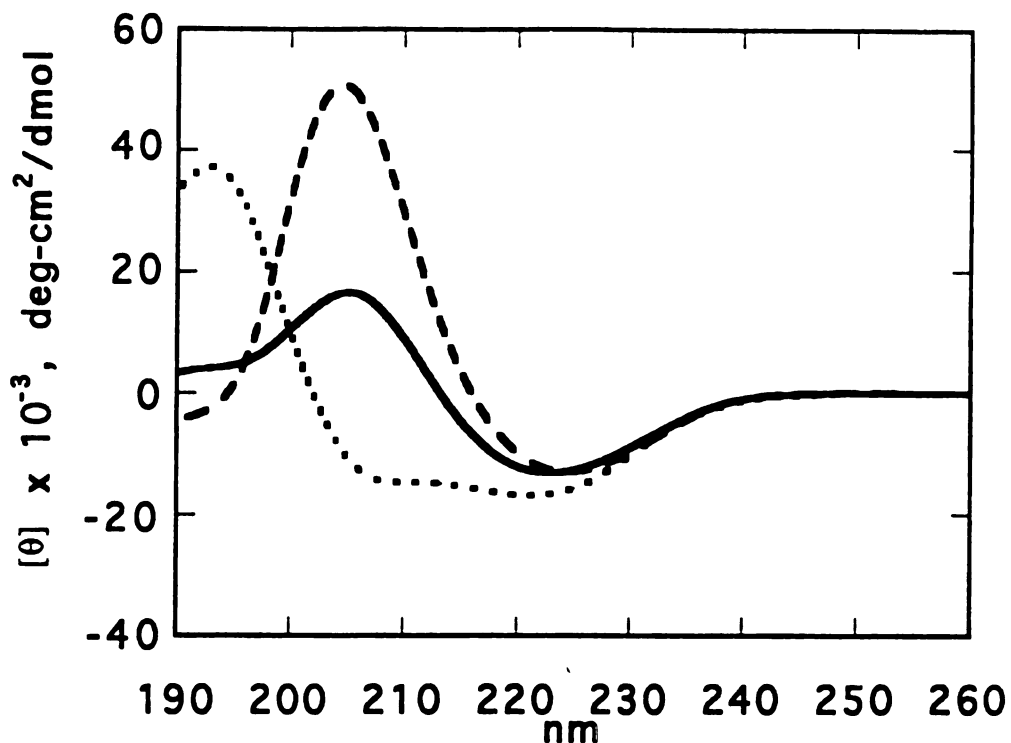


**Figure 13. Peptide I pH titration, 1.2 mM peptide concentration.** pH 6 (—); pH 8 (---); solution returned to pH 2 afterwards (·····). Spectra taken at 5°C. 100 mM NaCl/1 mM Na citrate/1 mM Na phosphate/1 mM Na borate buffer.

At higher pH's, the spectra have a single minimum that is significantly red-shifted; the position of the UV maximum is also red-shifted (Figure 13). Large amounts of precipitate were visible above pH 5; distortions due to light scattering may be affecting the spectra. Dropping the pH from 8 to 2 restored the alpha helical spectrum and caused most of the precipitate to re-dissolve (Figure 13).

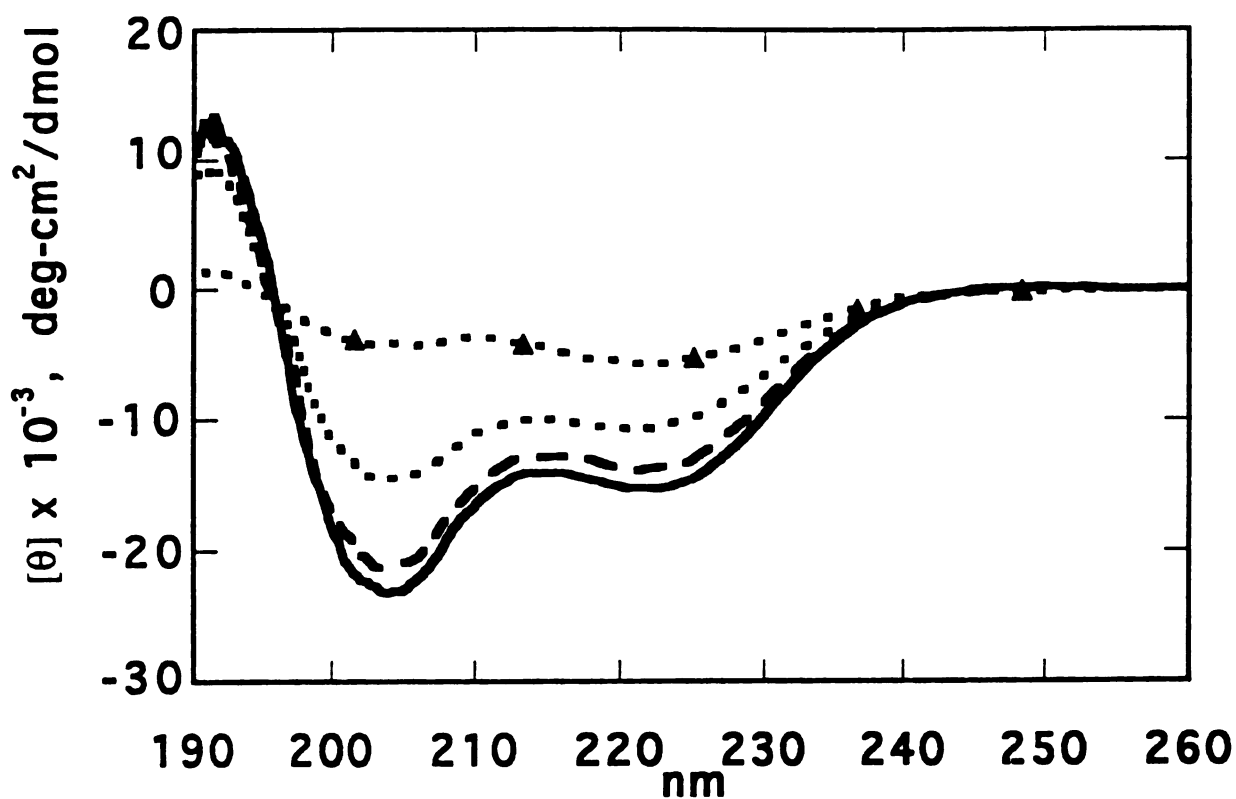


**Figure 14.** "Reverse" peptide I pH titration, 870  $\mu\text{M}$  peptide concentration. pH 11 (—); pH 10 (---); pH 9 (·····); pH 8 (-·-▲-·-). Spectra taken at 5°C. 100 mM NaCl/1 mM Na citrate/1 mM Na phosphate/1 mM Na borate buffer.

*"Reverse" pH titration of peptide I.* pH titration of "concentrated" peptide I in the "reverse" direction (starting at pH 11 and titrating to more acid pH) yields yet another set of distinct CD curves for the peptide (Figures 14-16). At pHs of 11 and 10, the peptide appears mostly helical, with an intensity at 222 nm comparable to that in the mid-pH range of the 100  $\mu\text{M}$  peptide I pH titration; at pH 9, the intensity of the 222 nm band drops to a similar value as that seen for the pH 8 CD curve in the 100  $\mu\text{M}$  titration. At pH 8, however, the

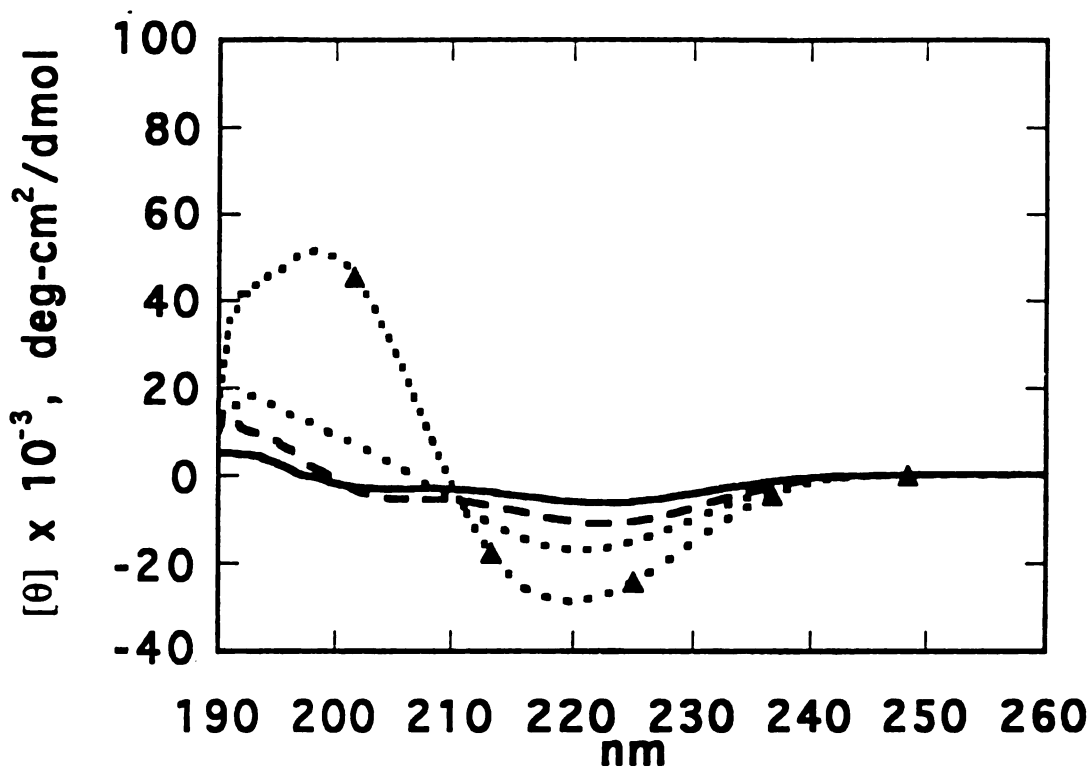


**Figure 15.** "Reverse" peptide I pH titration, 870  $\mu\text{M}$  peptide concentration. pH 7 (—); pH 6 (---); pH 5 (·····); pH 4 (-·-▲-·-). Spectra taken at 5°C. 100 mM NaCl/1 mM Na citrate/1 mM Na phosphate/1 mM Na borate buffer.

CD curve is very weak, and not suggestive of any typical structure. Precipitation is also occurring at this pH value, so the weak signal may be due to a lower concentration of peptide actually in solution.

The relatively featureless curve is also seen at pHs of 7 and 6 (Figure 15). At pH 5, a distinguishable minimum begins to appear at about 221 nm. Lowering the pH to 4 (Figure 15) increases the intensity of that minimum and causes a slight blue shift; a maximum near 200 nm also becomes apparent. Significantly, there is no evidence of a second minimum at 205 nm.

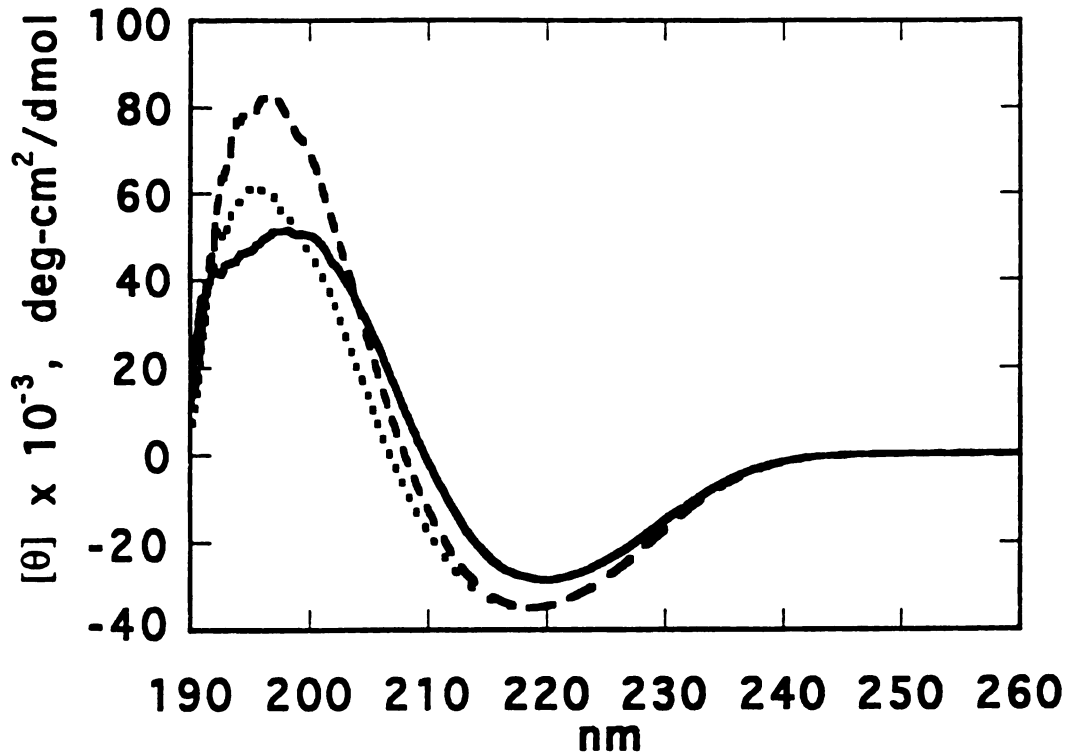


**Figure 16.** "Reverse" peptide I pH titration, 870  $\mu\text{M}$  peptide concentration. pH 4 (—); pH 3 (---); pH 2 (·····). Spectra taken at 5°C. 100 mM NaCl/1 mM Na citrate/1 mM Na phosphate/1 mM Na borate buffer.

Finally, upon dropping the pH to 3 and 2 (Figure 16), the single minimum is blue-shifted again, appearing at approximately 218 nm. The maximum is also blue-shifted below 200 nm, and the curves have the characteristic appearance of beta sheet.



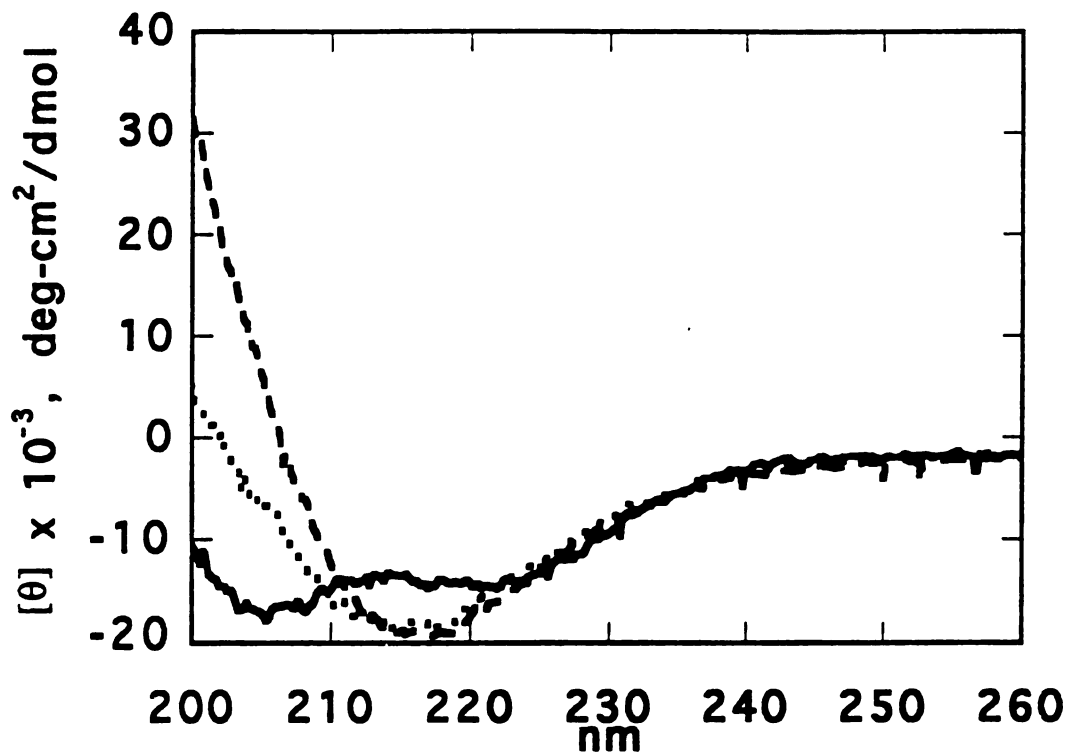


**Figure 17. Peptide II pH titration.** 300 $\mu$ M peptide concentration. pH 2.36 (—); pH 7.8 (·····); pH 5.5 (---). 15°C, in distilled water. Not baseline corrected. (Order of titration: starting pH 2.36; pH raised to 7.8; pH lowered to 2.5 [not shown, virtually identical to pH 2.36 curve]; pH raised to 5.5.)

*pH titration of peptide II.* Circular dichroism at selected pH values for peptide II, at 300  $\mu$ M peptide concentration, demonstrate alpha helical spectra at low pH and conversion to beta sheet at higher pH, as shown in Figure 17. These spectra were taken in distilled water, as peptide II structure is affected by NaCl concentration (see below). Similarly to the "forward" titration in peptide I, the alpha-to-beta transition in peptide II can be reversed by returning the solution to acidic pH.

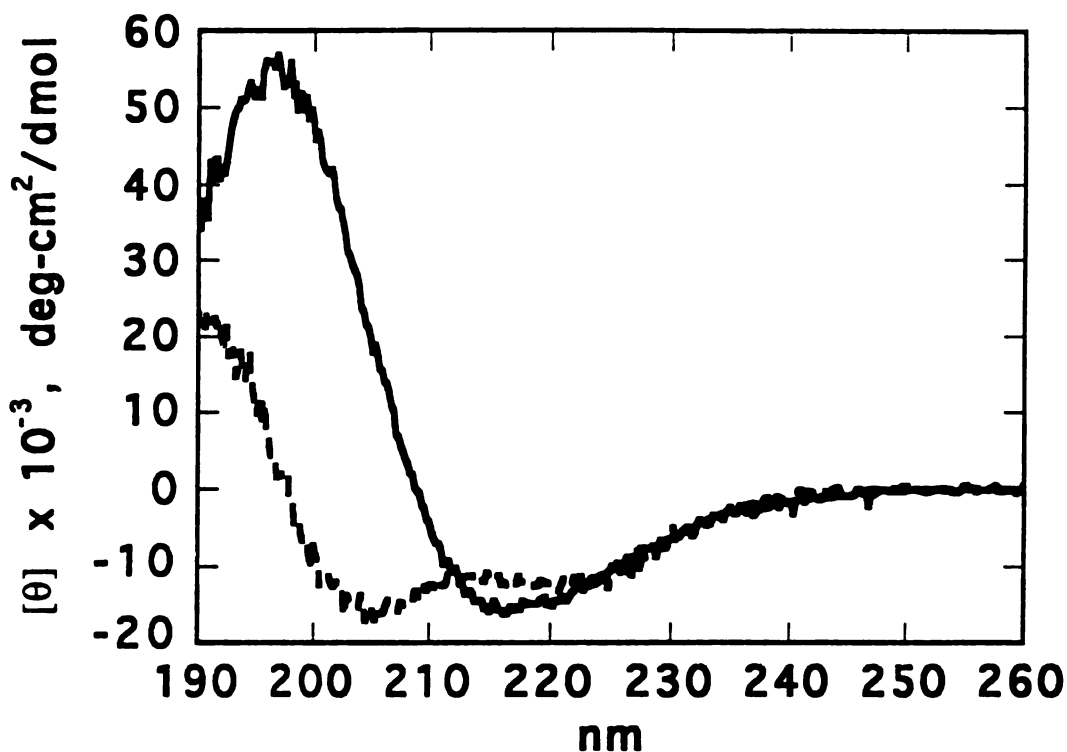


**Figure 18. Peptide II CD curves with and without salt present in solution.** 900  $\mu\text{M}$  peptide concentration, 10 mM Na phosphate buffer in D<sub>2</sub>O, 15°C. With 100 mM NaCl, pH\* 2.2 (—); no salt, pH\* 2.0 (---).

*Salt concentration effects on peptide II.* The conformation of peptide II is also affected by NaCl concentration. Figure 18 shows the CD spectra of peptide II in 10 mM sodium phosphate, with and without 100 mM NaCl added, at 900  $\mu\text{M}$  peptide concentration. In Figure 19, spectra taken at intermediate concentrations of salt are displayed.

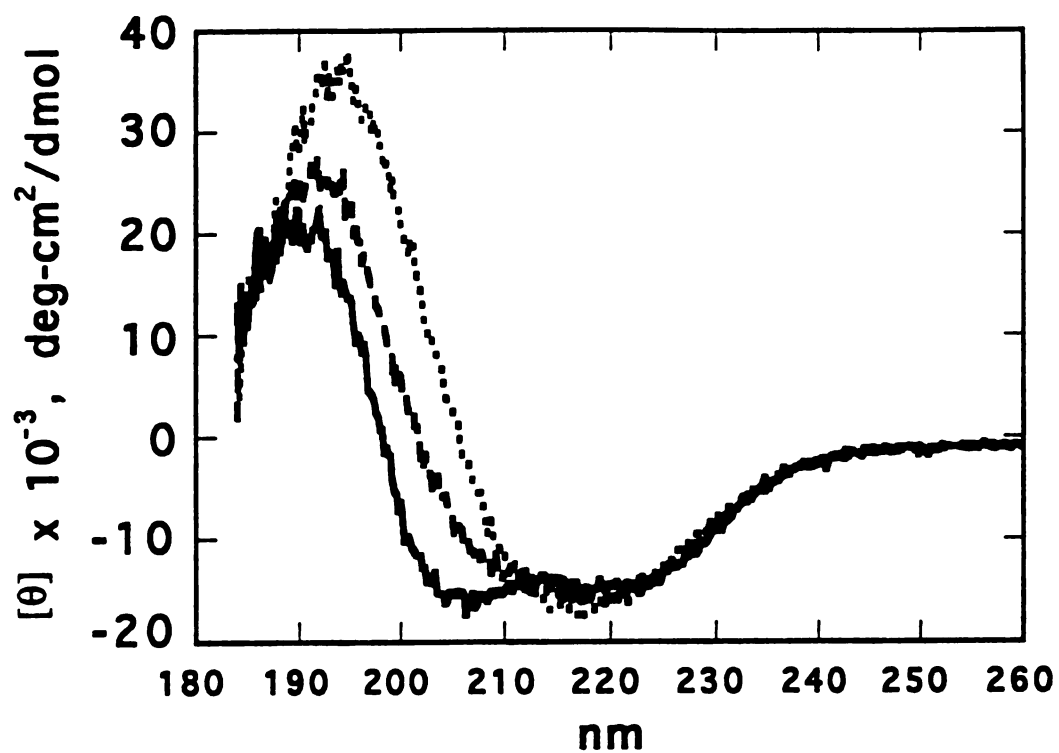


**Figure 19. Peptide II salt titration.** 800 $\mu$ M peptide concentration. 25 mM NaCl (—); 50mM NaCl (---); 75 mM NaCl (.....). 15 $^{\circ}$ C, pH\* 1.9 (in D<sub>2</sub>O), 10mM phosphate buffer. Not baseline corrected.

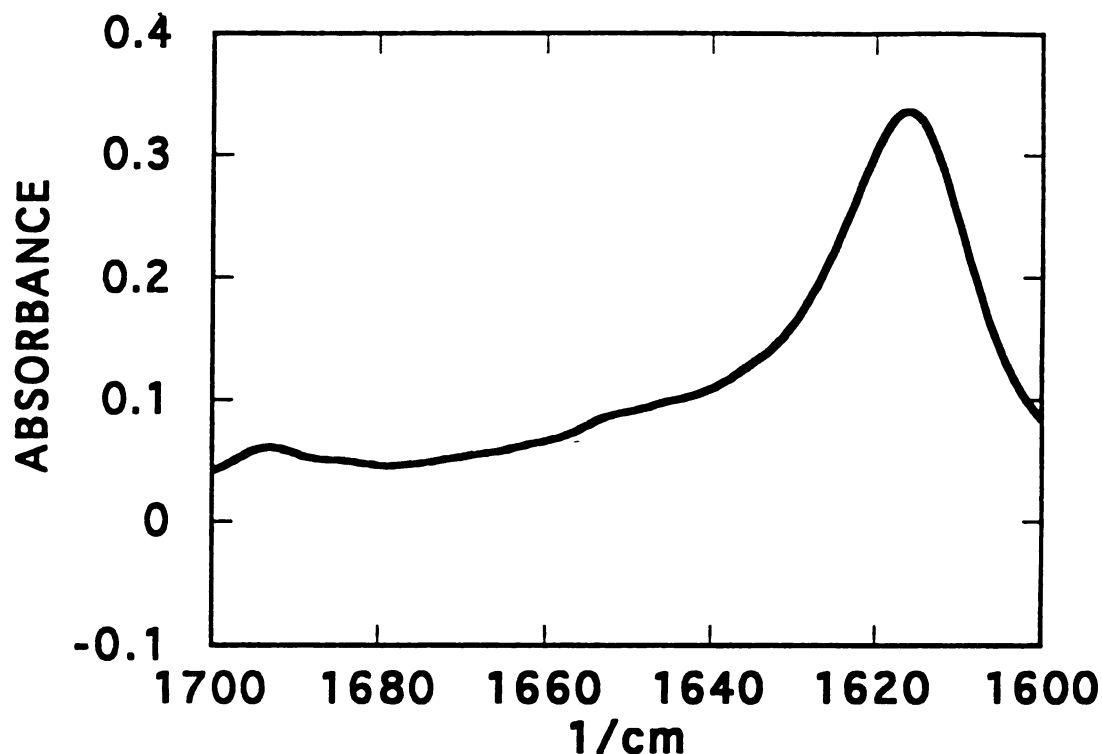


**Figure 20.** Fourier-transform infrared spectrum of peptide II. 4.5 mM peptide concentration, 100 mM NaCl concentration, 10 mM Na phosphate buffer. pH\* 2.01. Ambient temperature.

*Fourier-transform infrared spectra of peptide II with and without salt in solution.* In Figure 20, an FTIR spectrum of peptide II at 4.5 mM peptide concentration shows a low-frequency beta sheet band at  $1616\text{ cm}^{-1}$ , accompanied by a weak band at  $1694\text{ cm}^{-1}$ . In Figure 21, IR spectra of peptide II with and without salt present show a clear shift in the amide I' band. The sample containing salt shows an amide I' absorption peak at  $1612\text{ cm}^{-1}$ , a region assigned to low-frequency beta sheet. When no salt was present in the sample, the amide I' peak occurs at approximately  $1650\text{ cm}^{-1}$ , in the alpha helix/random coil region.

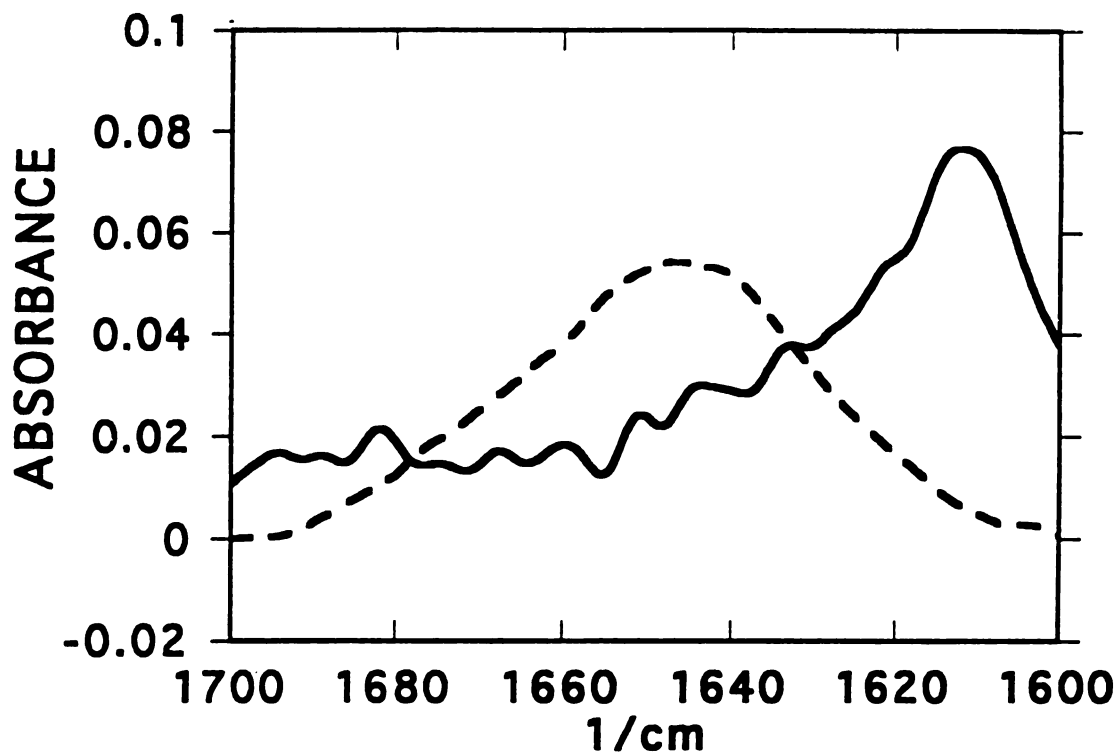


**Figure 21. Fourier-transform infrared spectra of peptide II, with and without NaCl. 900  $\mu$ M peptide concentration. With 100 mM NaCl (—); with no added NaCl (---). 10 mM Na phosphate buffer in D<sub>2</sub>O, pH\* 2.0, 15°C.**

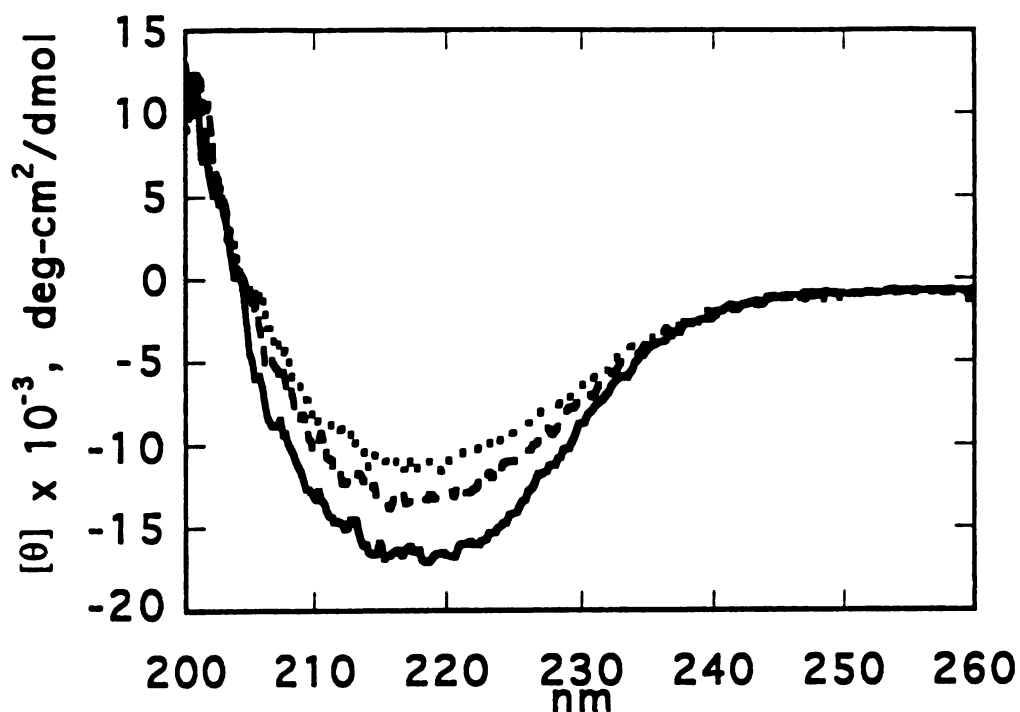


**Figure 22.** Temperature denaturation CD curves of peptide II. 75 $\mu$ M peptide concentration. 5 $^{\circ}$ C (—); 30 $^{\circ}$ C (---); 50 $^{\circ}$ C (.....). pH 2.4, 100 mM NaCl/1 mM Na citrate/1 mM Na phosphate/1 mM Na borate buffer. Not baseline corrected.

*Temperature effects.* Heating a solution of peptide II (peptide concentration of 75  $\mu$ M) in a buffer solution containing 100 mM NaCl yields the temperature denaturation curves shown in Figures 22 and 23. Even at 70 $^{\circ}$ C, there is a significant dip in the CD curve at 220 nm; this may be due to the intense UV transition of the azobenzene side chain in this region, although there may also be residual beta-sheet structure. After cooling the heated solution back to 5 $^{\circ}$ C, the spectrum displays the characteristics of an alpha helix. Over several

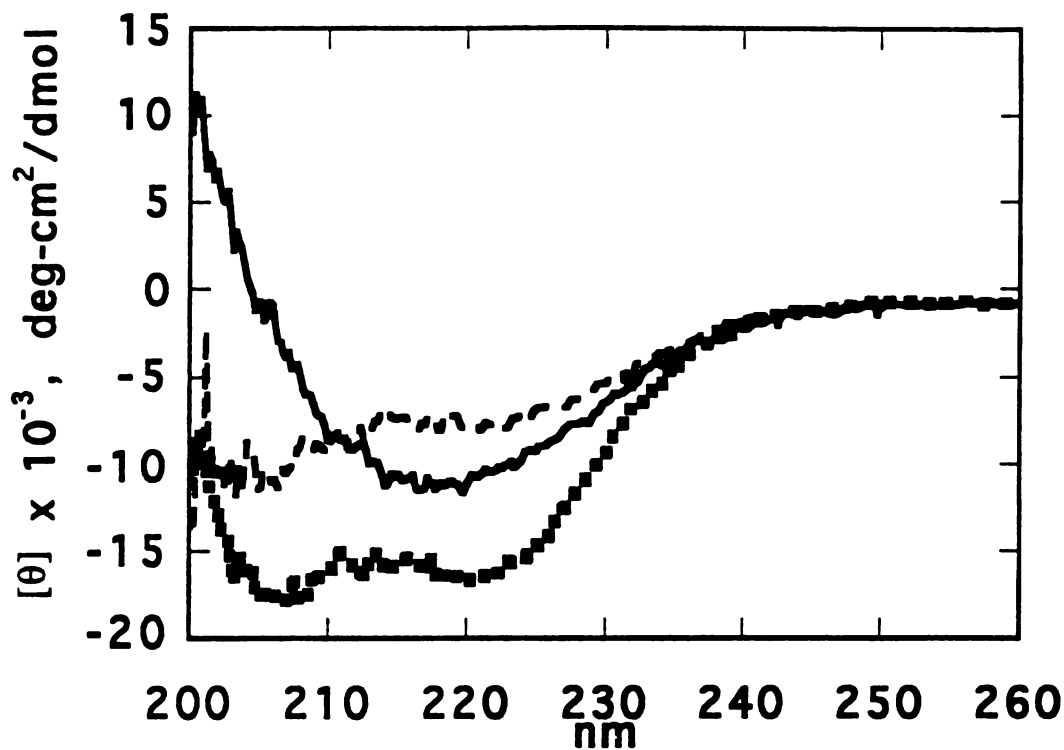


**Figure 23. Temperature denaturation CD curves of peptide II.** 75 $\mu$ M peptide concentration. 50°C (—); 70°C (---); solution returned to 5°C (cooled at room temp. over a one-hour period) (.....). pH 2.4, 100 mM NaCl/1 mM Na citrate/1 mM Na phosphate/1 mM Na borate buffer. Not baseline corrected.

months' time, the spectrum gradually changes back to the single-minimum spectrum characteristic of beta sheet (Figures 24-27).

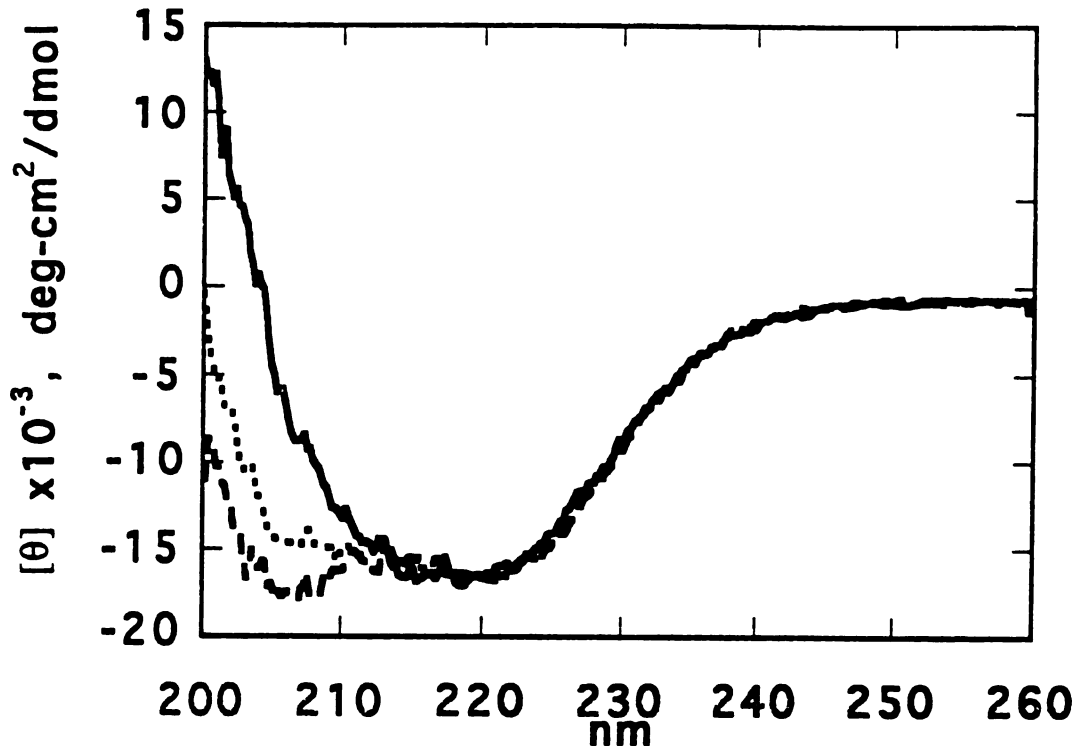


**Figure 24.** Time course of peptide II CD curves before, after heating. 75 $\mu$ M peptide concentration. Before heating (—); immediately after heating (---); 20 days after heating (····). All spectra taken at 5 $^{\circ}$ C. pH 2.4, 100 mM NaCl/1 mM Na citrate/1 mM Na phosphate/1 mM Na borate buffer. Not baseline corrected.

*Time course of peptide II CD curves after heating.* CD spectra of peptide II 20, 57, and 173 days after heating are shown in Figure 25. (Spectra before, immediately after heating, and 20 days after heating are shown in Figure 24). After 20 days, the solution displays a curve midway between the beta sheet curve before heating and the helical curve after heating. After 57 days, the peptide sample was filtered before taking the next CD time point. This resulted in a curve nearly identical to the original after heating curve, except for substantially



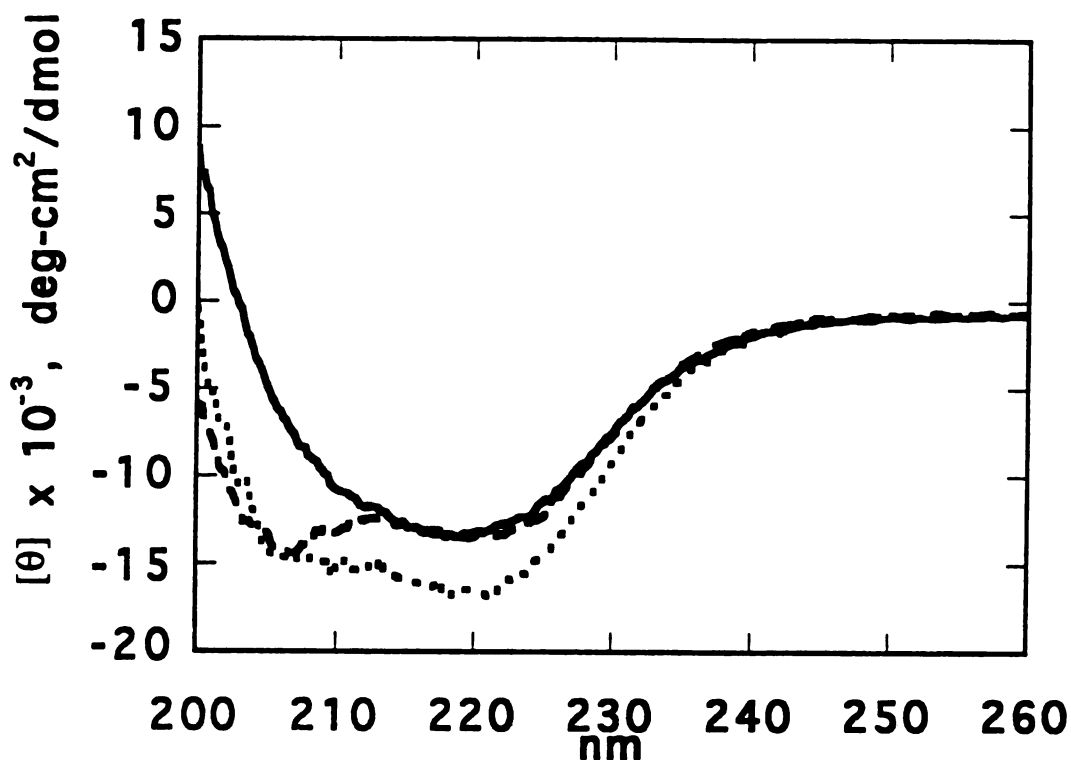


**Figure 25.** Time course of peptide II CD curves before, after heating. 75 $\mu$ M peptide concentration. 20 days after heating ( $\cdots$ ); 57 days after heating (FILTERED) ( $---$ ); 173 days after heating and 116 days after filtration ( $- \cdot -$ ). All spectra taken at 5 $^{\circ}$ C. pH 2.4, 100 mM NaCl/1 mM Na citrate/1 mM Na phosphate/1 mM Na borate buffer. Not baseline corrected.

lower intensity (Figures 24 and 26). After 173 days (116 days after the filtration), the peptide again displays a single-minimum beta sheet spectrum (the solution was not filtered prior to taking the 173 day time point). The 173-day spectrum is very similar to the spectrum taken before heating (Figures 24 and 27), although again there is a loss of signal intensity.

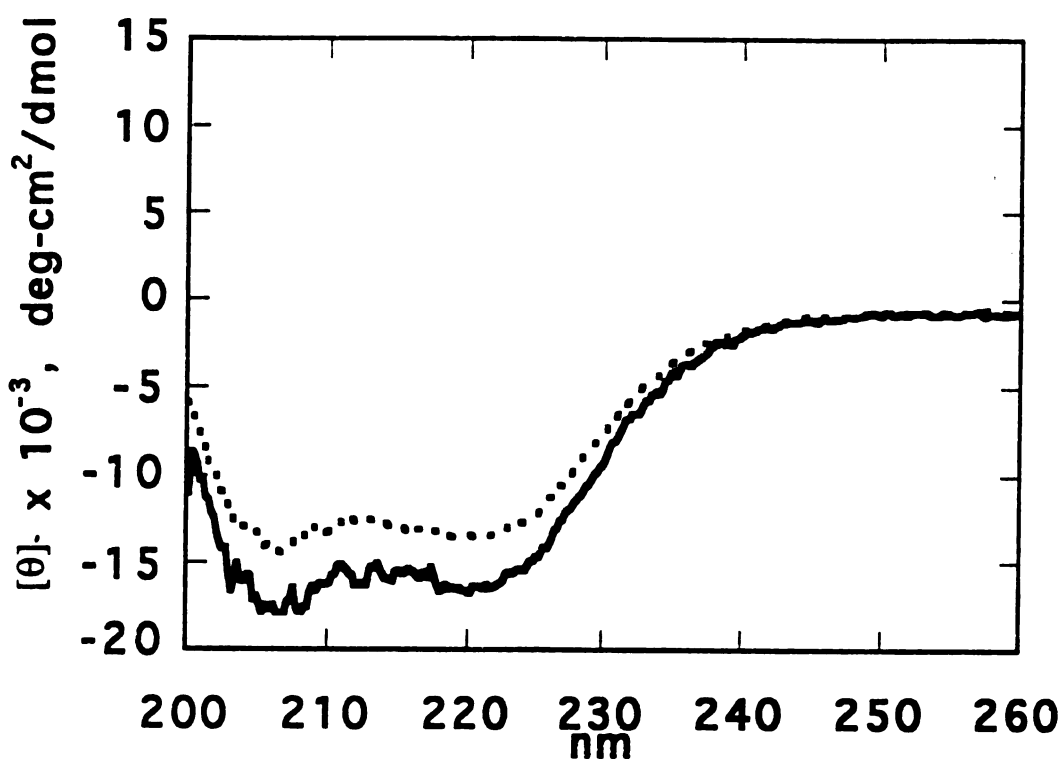


**Figure 26. Time course of peptide II CD curves after heating.** 75 $\mu$ M peptide concentration. Immediately after heating (—); 57 days after heating and immediately after filtration (·····). Spectra taken at 5°C. pH 2.4, 100 mM NaCl/1 mM Na citrate/1 mM Na phosphate/1 mM Na borate buffer. Not baseline corrected.

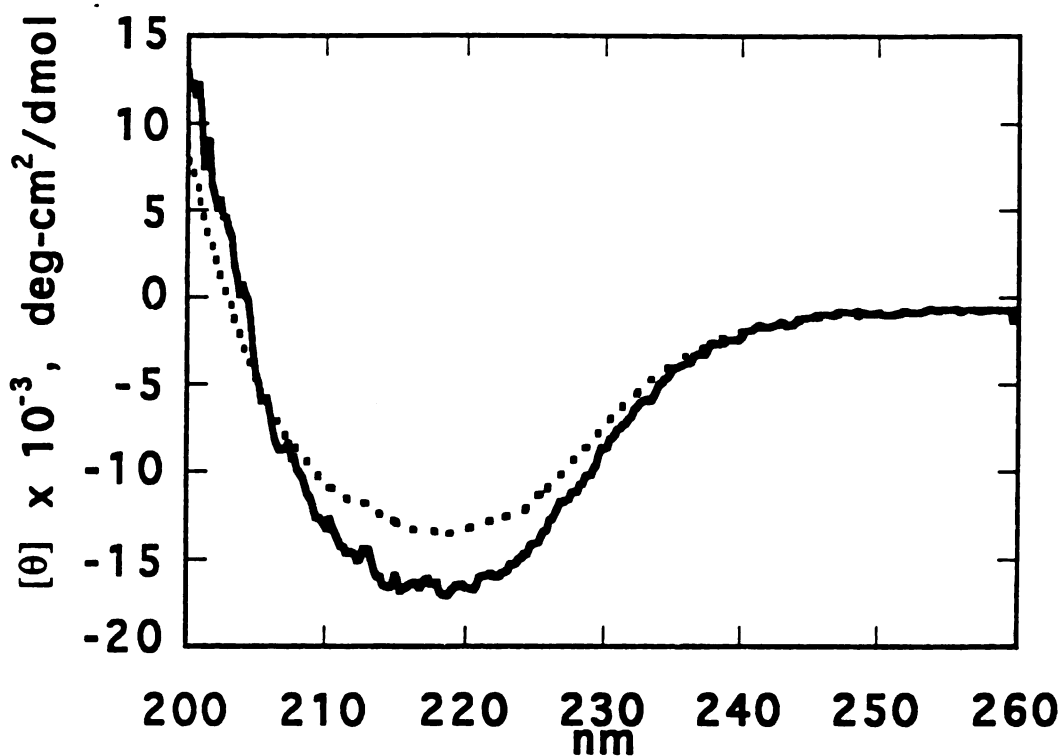


**Figure 27.** Time course of peptide II CD curves before, after heating. 75 $\mu$ M peptide concentration. Before heating (—); 173 days after heating and 116 days after filtration (·····). Spectra taken at 5°C. pH 2.4, 100 mM NaCl/1 mM Na citrate/1 mM Na phosphate/1 mM Na borate buffer. Not baseline corrected.

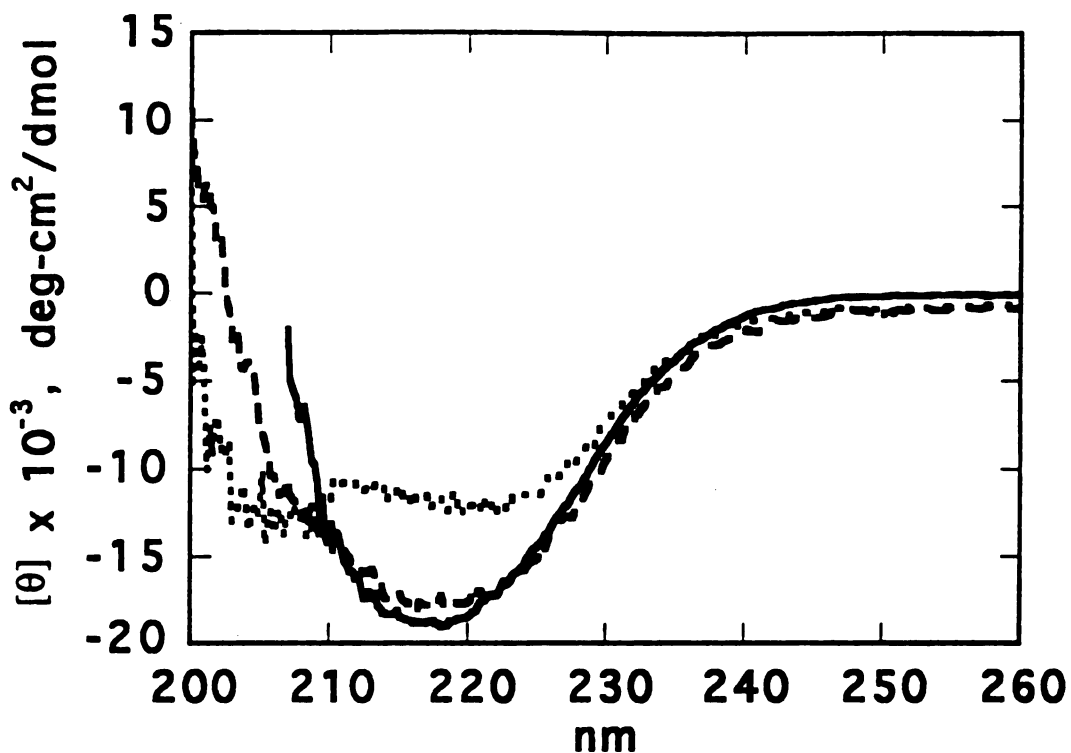


**Figure 28. Peptide II dilution CD curves.** Peptide concentrations of 376  $\mu\text{M}$  (—); 75  $\mu\text{M}$  (---); 7.5  $\mu\text{M}$  (.....). 5°C, in 100 mM NaCl/1 mM Na citrate/1 mM Na phosphate/1 mM Na borate buffer. pH 2.3 (376 and 75  $\mu\text{M}$ ); pH 2.2 (7.5  $\mu\text{M}$ ). Not baseline corrected.

*Concentration effects.* CD spectra of peptide II in 100 mM NaCl buffer solution at different peptide concentrations are shown in Figure 28. At the two higher concentrations, 375  $\mu\text{M}$  and 75  $\mu\text{M}$  peptide (at pH 2.3), the spectra have the single minimum at 218 nm characteristic of beta sheets. However, at the lowest concentration, 7.5  $\mu\text{M}$  peptide (pH 2.2), the spectrum has the double-minima appearance of an alpha helix.

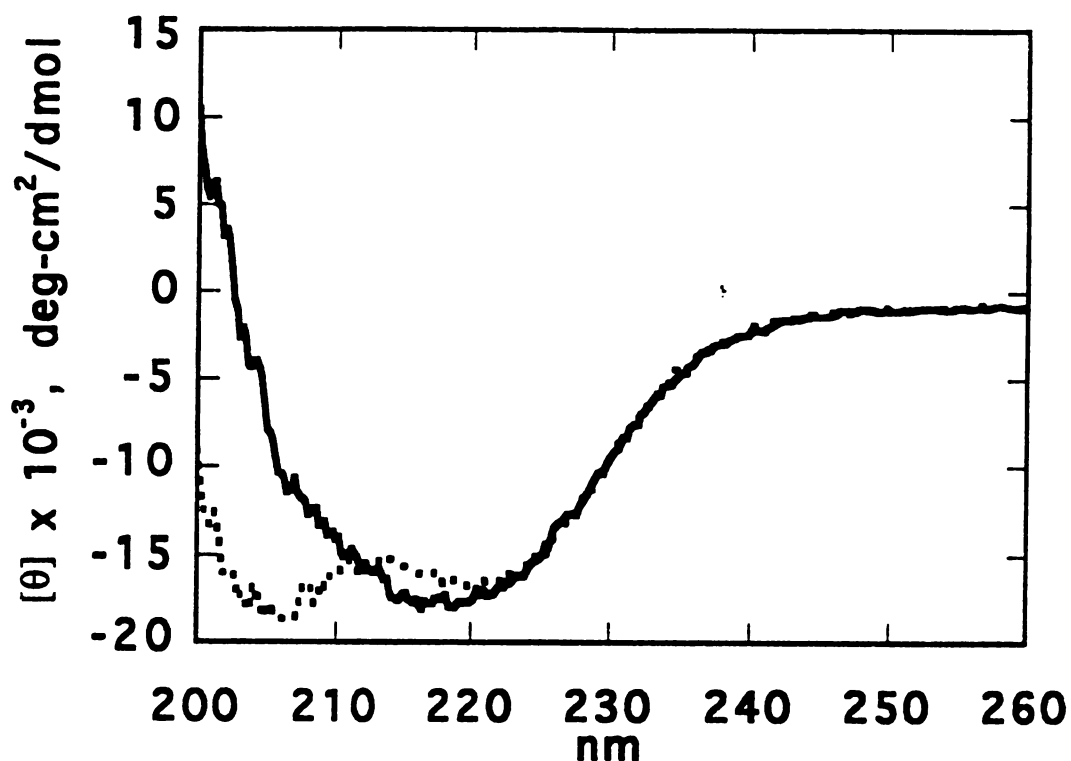


**Figure 29. Peptide II before and after UV irradiation.** 75  $\mu\text{M}$  peptide concentration. Before irradiation (—); 10 minutes after irradiation (·····). Spectra taken at 5°C. pH 2.4, 100 mM NaCl/1 mM Na citrate/1 mM Na phosphate/1 mM Na borate buffer. Not baseline corrected.

*Photoisomerization effects.* The CD spectra of 75  $\mu\text{M}$  peptide II are shown before and after irradiation with ultraviolet light (Figure 29). The peptide displays a single-minimum curve characteristic of beta sheet prior to exposure to UV light. After the 1-hour irradiation, the CD spectrum of the peptide displays the double-minima curve typical of helix. Storing the peptide solution in the dark for several weeks does not reverse the transition (Figure 30), unlike the behavior described above for peptide II after heating.

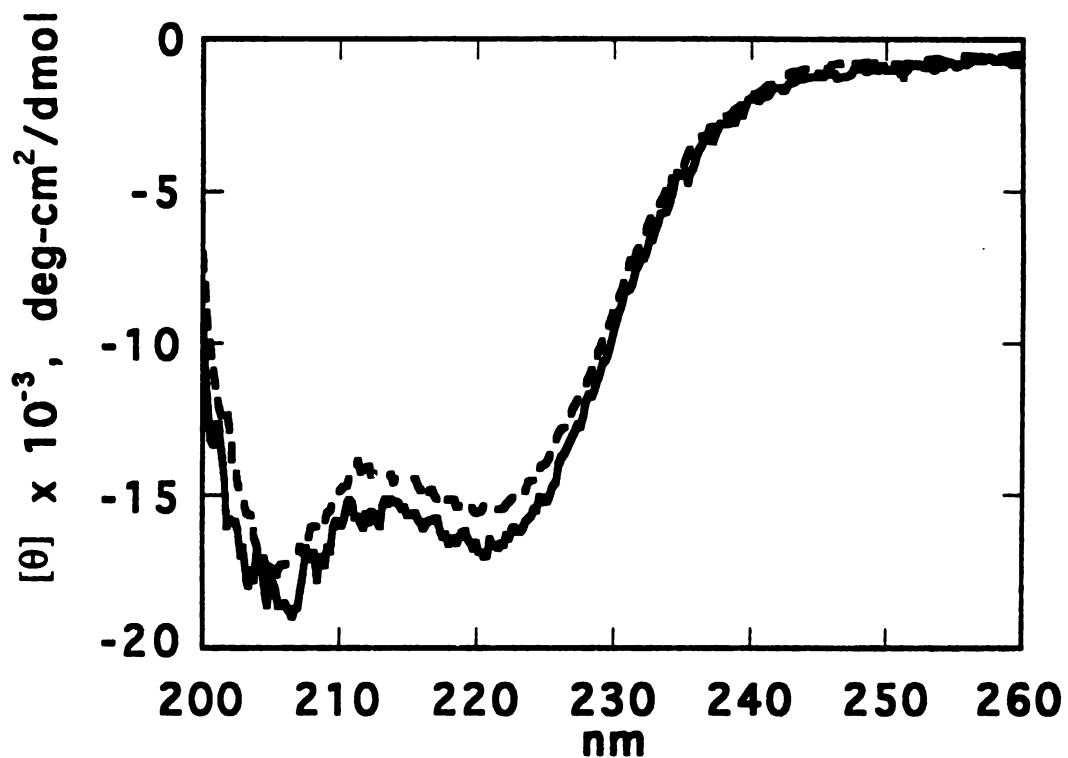


**Figure 30.** Time course of peptide II spectra after UV irradiation. 75  $\mu$ M peptide concentration. 10 minutes after irradiation (—); 67 days after irradiation (---). Spectra taken at 5°C. pH 2.4, 100 mM NaCl/1 mM Na citrate/1 mM Na phosphate/1 mM Na borate buffer. Not baseline corrected.

*Nuclear magnetic resonance spectra.* The fingerprint and amide regions of the NOESY spectrum of peptide I are shown in Figures 31 and 32, respectively. Resonance assignments are shown in Table I and are referenced to TSP. The spectrum is typical of helical peptides, as seen in the summary of observed NOEs in Figure 33, and is virtually identical to the spectrum found for a related peptide studied under similar conditions (Bradley et al., 1990). Fingerprint and amide regions of peptide II are shown in Figures 34 and 35, and residues with chemical shifts displaced by more than 0.05 ppm from their counterparts in peptide I are summarized in Table II. (The side chains of the lysines and of Thr-4 and Leu-9 could not be traced unambiguously in the NOESY spectrum because of the low peptide concentration needed to prevent aggregation of peptide II.) Of the amino acids common to both peptides I and II, only His-16 resonances are displaced by more than 0.1 ppm. Since the side chain of His-16 is in an *i, i+4* arrangement to the azobenzene side chain of Z-12, a change in the environment (and the chemical shifts) of the histidine is expected from the tyrosine to phenylalanylalanine mutation. The spectrum of peptide II contains fewer of the characteristic helical NOESY peaks expected, as shown in Figure 36. However, the lack of any significant difference between the chemical shifts of peptides I and II, combined with the helical NOEs observed for peptide II, indicates that peptide II is helical under the conditions studied.

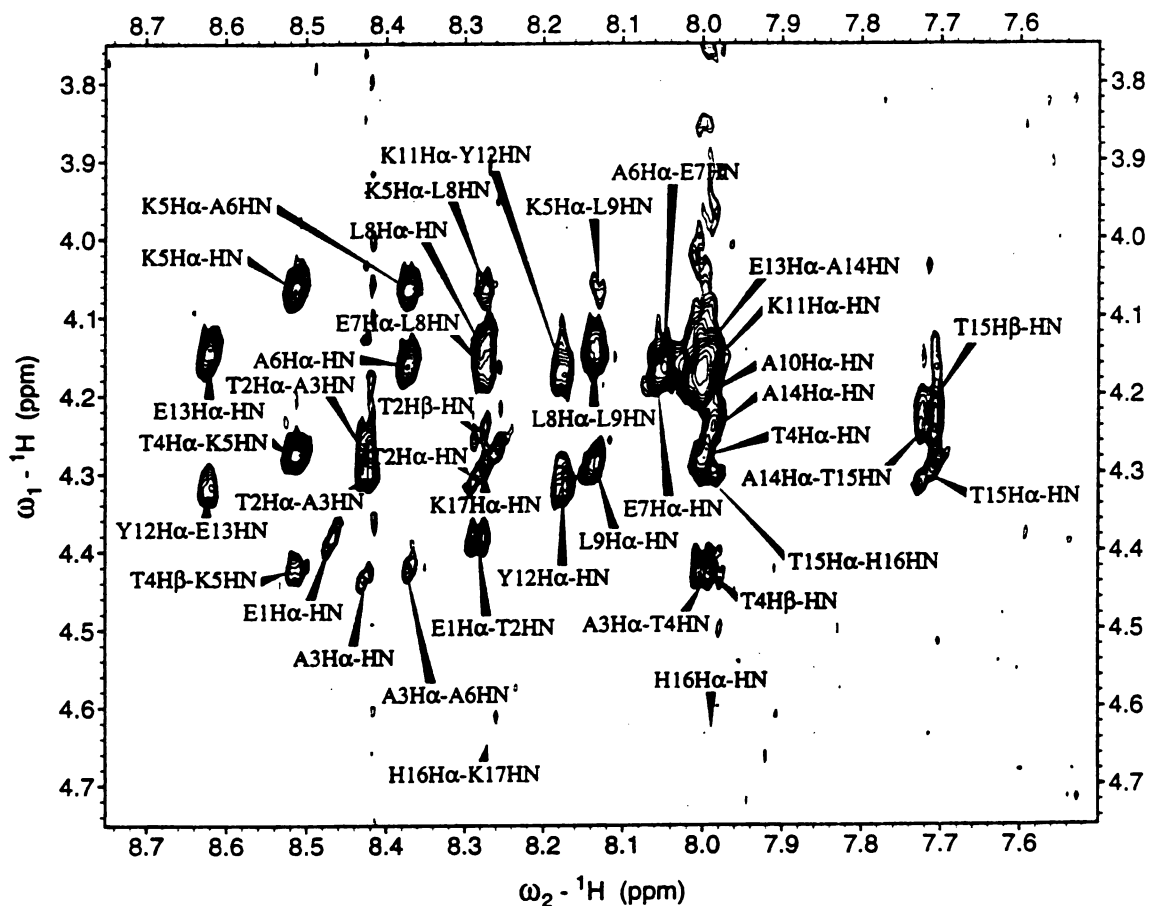


**Figure 31.** Nuclear magnetic resonance spectrum of peptide I recorded at 500 MHz, pH 2.4, 15°C. Fingerprint region of NOESY spectrum. (H16Ha-K17NH and K17Ha-NH, while not seen here, are marked based on their locations on the other side of the diagonal.)



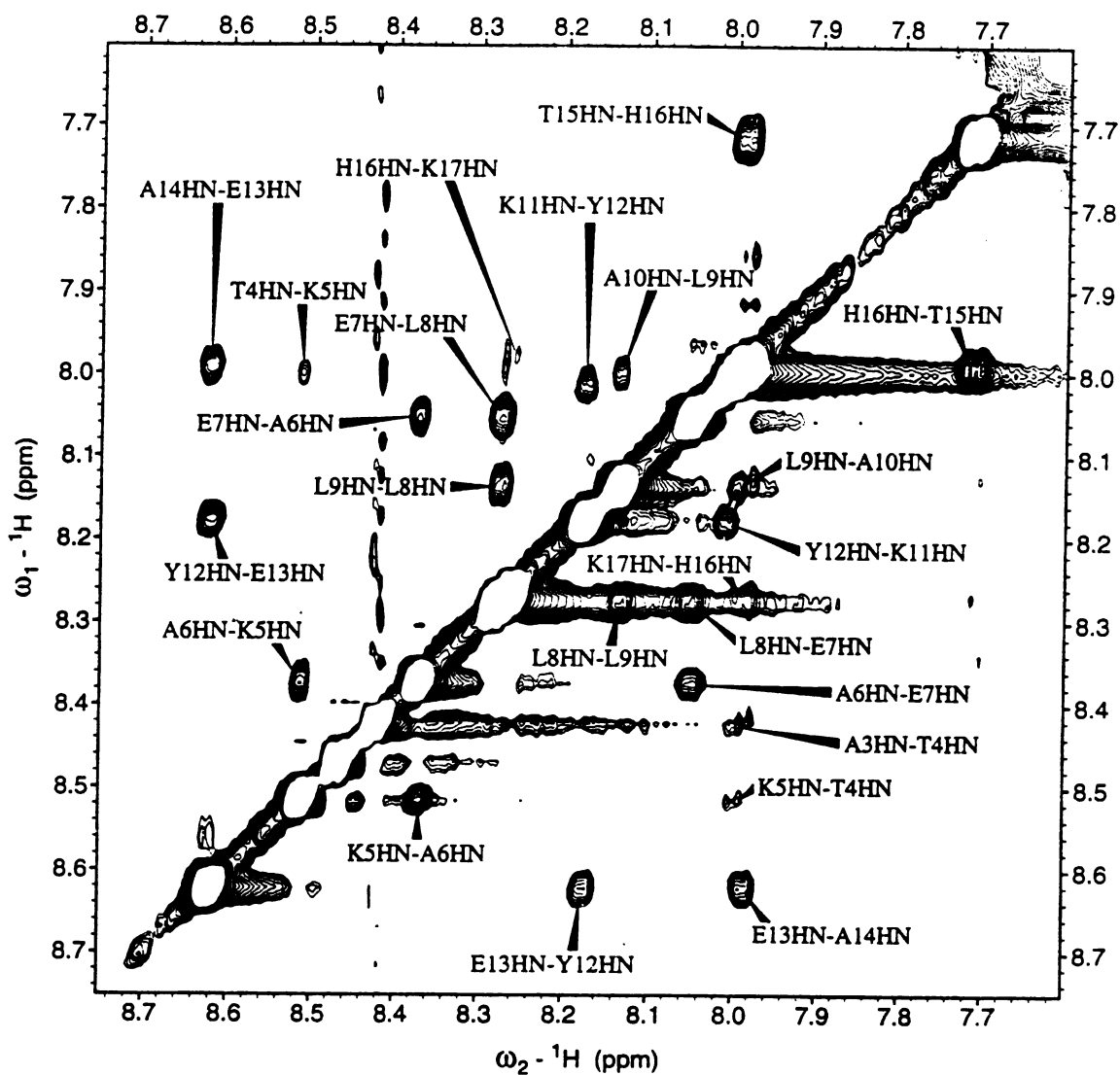


**Figure 32.** Nuclear magnetic resonance spectrum of peptide I recorded at 500 MHz, pH 2.4, 15°C. Amide region of NOESY spectrum.



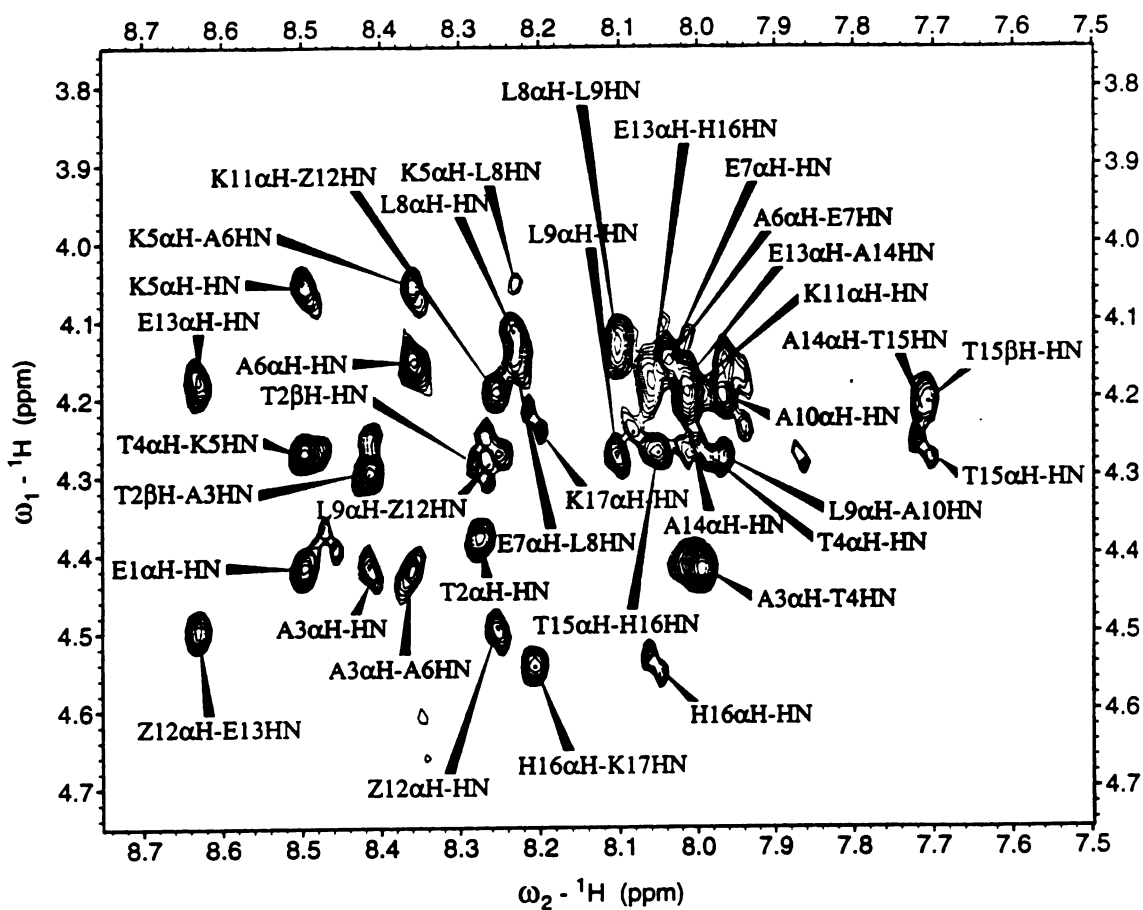


**Figure 34.** Nuclear magnetic resonance spectrum of peptide II recorded at 600 MHz, pH 2.4, 15°C. Fingerprint region of NOESY spectrum.

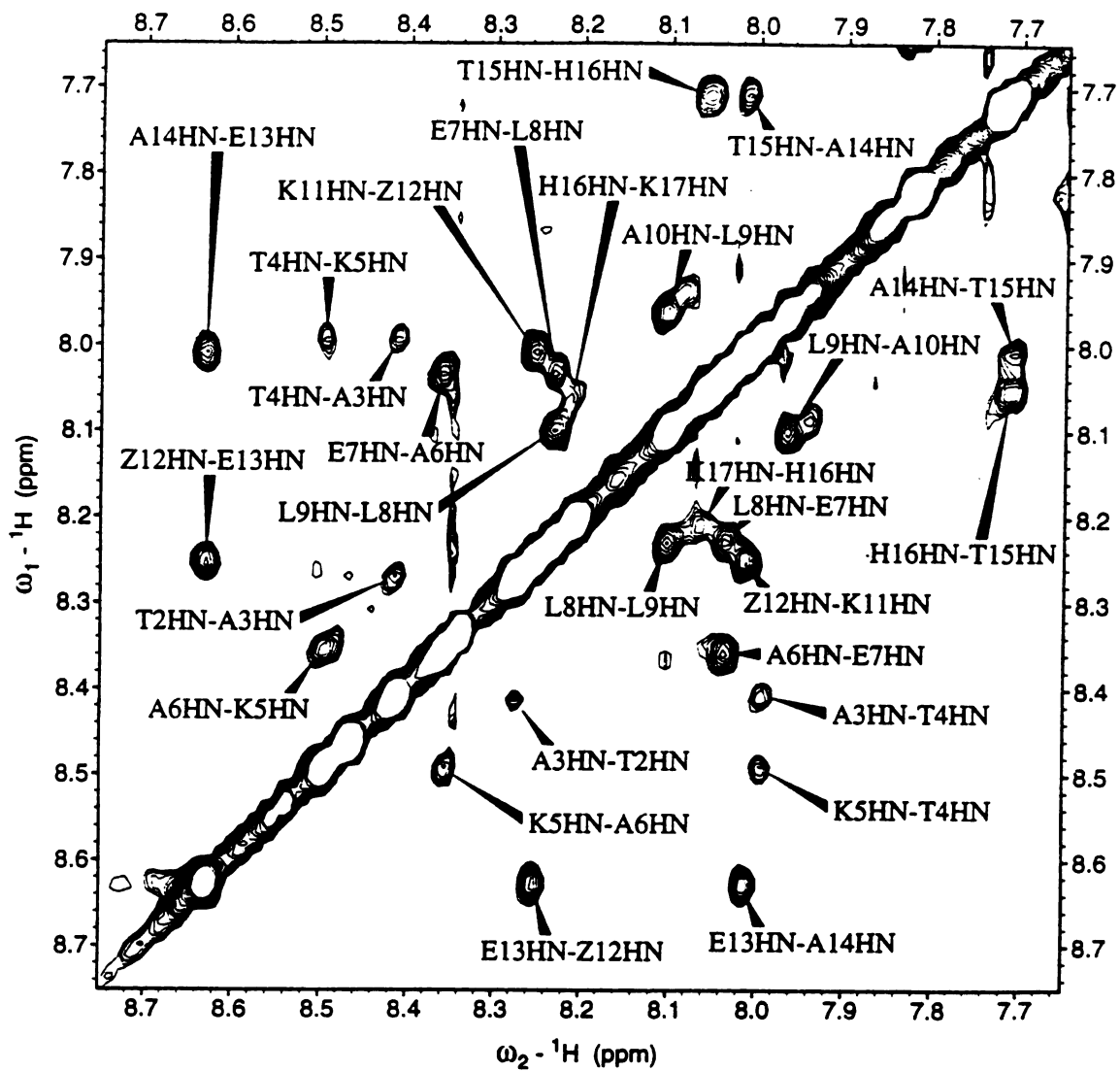


**Figure 35.** Nuclear magnetic resonance spectrum of peptide II recorded at 600 MHz, pH 2.4, 15°C. Amide region of NOESY spectrum.

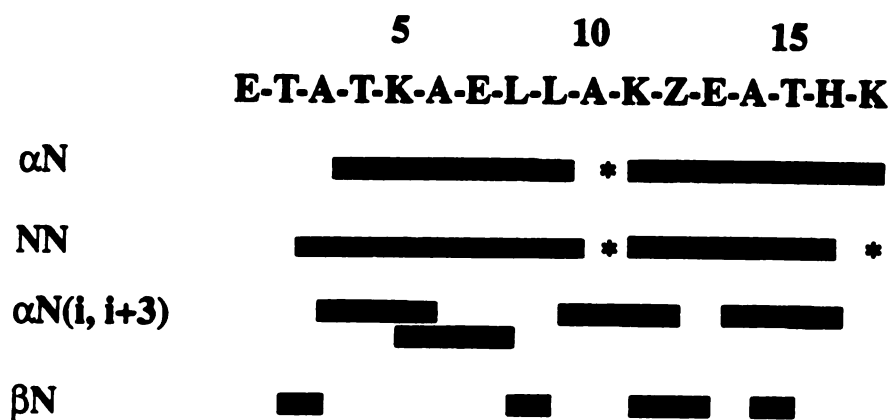


**Figure 36.** Summary of observed short and medium-range NOEs for peptide II. Regions where overlap prevented observation of an NOE are indicated by asterisks.

Table I. Resonance Assignments of Peptide I

Residue	NH	$\alpha$ H	$\beta$ H	$\gamma$ H	$\delta$ H	$\epsilon$ H	NeH	other
acetyl								
Glu-1	8.47	4.38	2.00	2.50				2.05
			2.11					
Thr-2	8.29	4.31	4.25	1.24				
Ala-3	8.43	4.43	1.43					
Thr-4	8.00	4.28	4.43	1.27				
Lys-5	8.51	4.07	1.86	1.45	1.71	2.99	7.59	
				1.57				
Ala-6	8.37	4.16	1.44					
Glu-7	8.05	4.17	2.13	2.54				
			2.23					
Leu-8	8.28	4.14	1.85	1.71	0.89			
Leu-9	8.13	4.29	1.71	1.62	0.89			
					0.94			
Ala-10	8.00	4.20	1.48					
Lys-11	8.00	4.17	1.89	1.39	1.68	2.98	7.59	
Tyr-12	8.18	4.32	3.15		7.05	6.65		
			3.22					
Glu-13	8.62	4.14	2.15	2.66				
Ala-14	7.99	4.24	1.51					
Thr-15	7.72	4.30	4.22	1.19				
His-16	7.99	4.64	2.79		8.43	7.18		
			3.20					
Lys-17	8.28	4.30	1.77	1.44	1.68	3.00	7.60	
amide	7.17							
	7.71							

**Table II. Resonance Assignments of Peptide II  
(> 0.05ppm  $\Delta\delta$  from Peptide I)**

Residue	NH	$\alpha$ H	$\beta$ H	$\gamma$ H	$\delta$ H	$\epsilon$ H	N $\epsilon$ H	other
Thr-2	8.27	4.38	4.30	1.23				
Z-12	8.25	4.50	3.36		7.42	7.72		*
His-16	8.05	4.54	2.76		8.34	7.04		
Lys-17	8.20	4.24	3.06		*	*	*	*

In summary, both peptides display more beta sheet character at higher peptide concentrations, higher NaCl concentrations, and at pH values of 5 or higher. Heating or photoisomerization of the azobenzene chain in peptide II disrupts the beta sheet character of the spectra.



## **DISCUSSION**

Understanding and interpreting the results presented requires consideration of several topics. Can the dramatic changes observed in the spectra be due to structural transitions? What information can be deduced about the conformations from the experimental data? Are there other plausible explanations for the experimental data? The dramatic changes in the spectra of the peptides under different conditions strongly suggest that the peptides are undergoing structural transitions. Evidence supporting this is considered below, and the conformational states most consistent with the data--an intermolecular beta sheet and a monomeric alpha helix--are discussed. The possibility that the changes in the spectra are due to experimental artifacts is also examined.

### **Nature of the Structural States**

The conformational states that are suggested most strongly by the spectra are, of course, alpha helix and beta sheet. This is the most obvious interpretation of the CD spectra, most of which are practically textbook examples of the secondary structure component curves. The data also strongly imply that the beta sheet form of the peptides is an aggregated state, while the helical form is monomeric. These conformations provide a straightforward and consistent

rationale for interpreting CD and IR experiments as a function of peptide concentration, salt concentration, pH, and temperature, as well as the change in the CD spectrum observed upon ultraviolet irradiation of peptide II.

The case for a monomeric alpha helix is examined first. The most powerful evidence of helical structure in the peptides are the nuclear magnetic resonance spectra, in particular the pattern of NOEs observed in the NOESY spectra of peptides I and II. The spectra were run in solutions of low pH and low salt, and the characteristic helical NOEs observed in the NMR experiments on peptides I and II (Figures 31-36), as well as in the parent peptide studied earlier (Bradley et al., 1990), clearly support an alpha helical conformation under these conditions. The remarkable similarity of chemical shifts among all the peptide spectra provides strong evidence that the structures are also very similar.

The *amount* of alpha helix present in the peptides poses a different problem. It is well known that helices tend to fray towards the termini; very few peptides have detectable helicity over their entire length (Chakrabarty et al., 1993a). In previous studies on this family of peptides (Bradley et al., 1990), it was demonstrated that most of the residues in helical conformation were contained in the latter half of the sequence. The very similar pattern of NOEs observed in peptide I suggests that the overall structure remains nearly the same (most of the unambiguous medium-range NOEs observed in the parent N, C-blocked (i, i+4) peptide were also observed in peptide I). From this it is fairly safe to conclude that the parts of the peptide not in helical conformation are in extended, or

random coil, conformation. Thus the state referred to here as "alpha helical" actually consists of a helix-coil equilibrium.

CD spectra of the helix state also suggests less than complete helicity. Estimates of the mean residue ellipticity at 222 nm of a completely helical polypeptide range around -33,000. The maximum ellipticity observed here for peptide I does not exceed -20,000. This indicates that not all chromophores are contributing to the helical signal. (Interference in CD spectra from aromatic residues is discussed below. While it is likely that aromatic contributions may cause some loss of intensity in the 222 nm minimum, it is unlikely that this accounts for the entire discrepancy in this small peptide system; see (Chakrabarty et al., 1993b).)

The postulated beta sheet structure relies entirely on CD and FTIR data for its spectral justification. Beta sheet peptides have been notoriously difficult to study by NMR. They tend to be aggregated to begin with, and over the several hours necessary for an NMR experiment may aggregate even further, causing broad linewidths and poor signal-to-noise ratios in the experiments. Solution state NMR experiments using the beta sheet forming solution conditions of peptide II were unsuccessful due to the broad linewidths observed (in most cases, the entire spectral window was filled with broad overlapping lines that completely obscured peak positions). For peptide I, large amounts of precipitate were often visible under the conditions where beta sheet was detected, indicating that attempts at NMR spectroscopy would be futile. These observations in and of themselves are useful, however, as they indicate that the peptide is

highly aggregated under these conditions, an indirect piece of evidence for the postulated beta sheet aggregate.

The most suggestive direct evidence for the beta sheet aggregate comes from the CD experiments as a function of peptide concentration. An aggregate would be favored at higher concentration, whereas lower concentration would disfavor aggregation. In the spectra in Figure 28, beta sheet is observed at higher concentration and alpha helix at lower concentration. This suggests that the aggregated beta sheet dissociates into monomeric helix when the concentration drops.

Beta sheets come in both parallel and antiparallel arrangements. The antiparallel sheet structure has stronger hydrogen bonds and would be the most likely candidate for the sheet structure here. The design of the peptide, where oppositely-charged side chains can align in salt bridges only in the antiparallel arrangement, also points towards antiparallel sheet (parallel sheet structure would require like charges on side chains to be aligned). Finally, the FTIR spectrum of peptide II at high concentration (Figure 20) shows a weak band at  $1696\text{ cm}^{-1}$ . IR spectra of antiparallel beta sheet tend to have such a weak band at high wavenumber, while no such band is observed in parallel beta sheet. The band here is observed at somewhat higher wavenumber than usual. However, due to the unusually low wavenumber of the main beta sheet band at  $1616\text{ cm}^{-1}$ , it is not implausible that the extra splitting has shifted the weaker secondary band out of the usual range. Estimates of the "usual range" of this band tend to vary; different researchers assign it to the regions  $1678\text{-}1672\text{ cm}^{-1}$  and  $1689\text{-}1682\text{ cm}^{-1}$ . A similar

antiparallel beta sheet aggregate structure has been proposed for an amphiphilic peptide that forms a highly stable beta sheet (Zhang et al., 1994).

This model also accounts for the results observed in the "forward" pH titration and the salt titration. The pH titration of peptide I at 1.2 mM concentration suggests that the peptide forms an alpha helix at pH 2, where the peptide carries a net charge of +4, which would disfavor aggregation. As the pH rises and the glutamic acid residues begin to deprotonate, the alpha helical spectrum becomes distorted; at pH 5, where most of the glutamic acid residues are negatively charged, the peptide carries a net charge of +1 and has less electrostatic repulsion to overcome to form an aggregate. This aggregation event occurs at much lower concentration in peptide II than in peptide I. At 100 uM peptide concentration and 100 mM NaCl concentration, peptide I displays a (partially) helical conformation at all pH values. Peptide II, however, gives rise to a beta sheet CD spectrum at 75 uM peptide concentration at pH 2.3, 100 mM NaCl concentration.

The aggregated beta sheet/monomer alpha helix model also provides a straightforward explanation of the NaCl titration results and heating experiment. Peptide II, like peptide I, has a net charge of +4 at low pH. Increasing the amount of salt present in solution screens the charge on the peptide more effectively, facilitating formation of the aggregated beta sheet as observed in Figures 18 and 19. Similarly, heating the peptide II solution could lead to disaggregation of the beta sheet complex into extended monomers at higher temperatures. Upon cooling, the peptide would adopt the

preferred monomeric conformation of alpha helix. This conclusion is further supported by the time course of the peptide spectra after heating and cooling (Figures 22-27). 20 days post-heating, the peptide spectra appears intermediate between sheet and helix. Filtering the solution after 57 days, however, caused reversion to a helical spectrum, with substantial loss of signal intensity. The most logical explanation for this behavior is that beta sheet aggregates large enough to be trapped in the filter pores were removed from solution, while the monomeric helix form was not filtered out of solution.

While this model accounts for most of the experimental data, the "reverse" pH titration (Figures 14-16) indicates that, at low pH, peptide I does not necessarily form an alpha helix. This would imply that either the helical state observed at pH 2 for the forward titration, the sheet state observed at pH 2 for the reverse titration, or both, are not thermodynamic endpoints, since the state of the system is not identical despite very similar conditions (the major difference is a 25% difference in peptide concentration). This implicates a kinetic phenomenon. Such a mechanism is reasonable to invoke in light of the time course seen after peptide II heating, where the helical structure at low pH gradually converted to beta sheet form.

In exploring this kinetic hypothesis, some conjectures on the state of the peptide at various stages may aid in understanding the structural transitions. When the peptide is cleaved off the resin with trifluoroacetic acid, it is unlikely that any structure is present in this highly denaturing solvent, and the peptide would be monomeric and randomly structured. Upon evaporating the TFA, the peptide would

carry several positive charges (three on lysine and one on histidine), with associated TFA anions. After redissolving the peptide in water, the peptide would still carry several positive charges and would be unlikely to aggregate quickly; however, the peptide is no longer in a denaturing solvent, and presumably can form alpha helices in the crude state. Reverse-phase liquid chromatography, in water/acetonitrile mixtures, is somewhat denaturing, but there is evidence of helical structure in peptides during HPLC purification, and it is reasonable to assume that the peptides are still monomeric and helical during and after HPLC purification, when they are lyophilized out of the water/acetonitrile mixture. Since the HPLC solvents are at low pH (approximately 2), again the peptides would be unlikely to aggregate.

The next step in the structural analysis is dissolving the peptide in CD buffer (100 mM NaCl/1mM Na phosphate/1 mM Na citrate/1 mM Na borate) and adjusting the pH. This generally takes 5-10 minutes. Both the forward and reverse pH titrations thus start with the peptide in a highly charged state (+4 when starting at low pH, -3 when starting at high pH), and most importantly, *the peptide has not been in an unstructured state for any significant length of time.*

In the forward pH titration, the peptide switches from helical to sheet, and shows evidence of structure at all pHs. Dropping the pH from 8 to 2 causes the peptide to revert from sheet form to helical form. In the reverse titration, the peptide switches from helical at high pH to essentially unstructured in the midrange of pH. It is possible that beta sheet is the more stable structure of the peptide,

even at low pH, and that a large, extended sheet structure can assemble rapidly from the unstructured conformation seen at the mid-pH range in the reverse titration. The beta sheet conformation seen in the forward pH titration, however, had to form from helical precursors. Since the peptide had to first unfold, and then assemble into sheets, the sheets in the forward titration may be smaller aggregates than those in the reverse titration, since they had less time to form. These smaller sheets formed in the forward titration may then be more prone to dissociation at lower pH values than the sheets formed in the reverse titration.

While the above scenario is plausible, it must be stressed that it is based solely on supposition, and not on direct experimental evidence. Performing experiments to test the hypothesis could be quite problematic, as very small differences in starting conditions may lead to very divergent kinetic results.

### **Significance of the Conformational Transition**

Whatever the explanation advanced for the "reverse" pH titration, it is clear that the conformations of peptide I and peptide II are influenced by a wide variety of solution conditions. The fact that a single peptide can adopt two very different secondary structures based on the solution environment carries important implications for biological systems and for protein design and engineering. Earlier work has shown that peptide conformation is affected by solution additives such as trifluoroethanol and sodium dodecyl sulfate



(Mutter and Hersperger, 1990; Reed and Kinzel, 1993; Waterhous and Johnson, 1994; Zhong and Johnson, 1992) and interface effects (Taylor et al., 1993). In the experiments presented here, we show that peptide concentration, pH, and salt concentration also play a role in determining peptide structure. From a biological perspective, the most significant of these factors are the salt concentration and pH; physiological systems often contain environments of different ionic strength or pH separated by membranes, which may influence peptide and protein structures in those environments. The salt concentrations used here are well within the limits encountered in living systems (ca. 150 mM (Alberts et al., 1994)). Understanding how and why peptides aggregate may have important biological implications, as the conversion of an alpha helical peptide or protein into an aggregated, insoluble beta sheet form may account for the pathology observed in Alzheimer's disease and scrapie (Nguyen et al., 1995; Zagorski and Barrow, 1992).

The photoswitch behavior of peptide II is of distinct interest, since it enables the study of a conformational switch triggered by the rapid *trans*-to-*cis* azobenzene photoisomerization. Other peptides containing phenylazophenylalanine (Goodman and Kossoy, 1966) or azobenzene (Pieroni and Fissi, 1992) side chains have been studied; many of these peptides also display changes in secondary structure upon irradiation. An important difference should be noted between the previous systems and the peptide studied here which renders peptide II particularly useful. The systems used in previous experiments were typically high molecular weight polymers, with a large percentage of azobenzene incorporated into each peptide chain.

In contrast, peptide II is relatively short and contains only one azobenzene residue, making it much more feasible to study the peptide and to examine the effects of replacing individual residues on the structural transition.

## **Spectroscopic Considerations**

An important caveat that must be considered in any interpretation of our results is the possibility that spectral artifacts, not true conformational transitions, account for the beta sheet and alpha helix spectra. Aromatic residues, such as tyrosine and tryptophan, are known to distort the circular dichroism spectra of peptides and proteins, due to overlap of electronic transitions from the peptide bonds and the aromatic rings (Chakrabarty et al., 1993b; Vuilleumier et al., 1993; Woody, 1994). The azobenzene side chain has particularly strong electronic transitions in the peptide bond region, which requires caution in interpreting CD spectra. Infrared spectroscopy utilizes a different physical property of the peptide bond than CD, making it unlikely that artifacts will be mistaken for true conformational changes in both types of spectra. The weak azobenzene stretching frequency occurs outside of the amide I' region, and is unlikely to affect the results of the FTIR experiments (Williams and Fleming, 1980). The experiments with the peptides at different concentrations also lends support to the aggregate/monomer hypothesis. Since the concentration of the peptides dramatically affects the spectrum obtained, the CD spectra

almost certainly arise from a true aggregation event, not from artifacts due to the aromatic side chains. Finally, NMR provides yet another independent physical method of determining conformation, and the strongest evidence for the helical state of the peptides. Attempts at acquiring NMR spectra using the beta sheet-forming conditions were unsuccessful due to extremely broad linewidths (data not shown). While this prevents solution NMR structure determination under those conditions, it also provides another piece of evidence that an aggregation event is occurring during the structural transition, as discussed above.

Two interesting aspects of the CD spectra presented here merit comment. The first aspect is the relative intensity of the minima of helix and sheet in Figures 12, 13, 17, 18, 19, 24, 28 and 29. The spectrum of an alpha helix tends to have a minimum approximately twice as strong as a beta sheet spectrum, as observed in the pure component spectra for polylysine (Greenfield and Fasman, 1969). The spectra of alpha helix and beta sheet presented here have roughly equal intensities at their minima. A reasonable explanation for this phenomenon is that the beta sheet conformation places a larger percentage of the peptide bond chromophores in ordered secondary structure than the alpha helical conformation. It is also possible that the azobenzene electronic transitions discussed above, while not strong enough distort the qualitative information contained in the CD spectra, affect the magnitude of the spectra associated with alpha helix and beta sheet. A second unusual aspect of the CD spectra is observed in Figure 13, where both the  $n-\pi^*$  and  $\pi-\pi^*$  transitions of the beta sheet spectra observed at pH 6 and 8 are red-

shifted, and the intensities of both beta sheet transitions are stronger than those of the same transitions in the alpha helix. Such a red shift and enhanced intensity have been calculated for model polyvaline beta sheet spectra (Manning et al., 1988), and are attributed to the strong twist in the sheet caused by the beta-branched side chains of valine. It is possible that the presence of the three threonine residues are causing similar phenomena to occur in our spectra. Other researchers have also noted unusually high intensities for the  $\pi$ - $\pi^*$  transitions. Those transitions were blue-shifted instead of red-shifted, but were believed to be due to stacking, not twisting, of beta sheets (Cort et al., 1994).

## **Conclusions**

The data presented here adds to the diversity of conformational behavior observed in peptides. Our peptide design provides an excellent system for studying beta sheet-alpha helix conformational switching. Mutation of residues can illuminate the dependence of the conformational switching behavior on specific amino acids. Experiments with a variety of salts and solution additives can yield thermodynamic data for the conformational switch under different solution conditions. Finally, the photoswitch behavior of peptide II can be utilized for studying the kinetics of secondary structure interconversion. Rapid spectroscopic techniques have been developed which can detect such changes on nanosecond (Zhang et al., 1993) and picosecond (Lewis et al., 1992; Stoutland et

## REFERENCES

Alberts, B., Bray, D., Lewis, J., Raff, M., Roberts, K. and Watson, J.D. (1994). *Molecular Biology of the Cell*. Garland Publishing, Inc., New York.

Anfinsen, C.B., Haber, E., Sela, M. and White, F.H. (1961). *Proc. Natl. Acad. Sci. USA*. **47**, 1309-1314.

Atherton, E. and Sheppard, R.C. (1989). *Solid Phase Peptide Synthesis: A Practical Approach*. Practical Approach Series. IRL Press, New York.

Brack, A. and Spach, G. (1981). *J. Am. Chem. Soc.* **103**, 6319-6323.

Bradley, E.K., Thomason, J.F., Cohen, F.E., Kosen, P.A. and Kuntz, I.D. (1990). *J. Mol. Biol.* **215**, 607-622.

Brown, C.J. (1966). *Acta Crystallographica*. **21**, 146-152.

Brown, J.E. and Klee, W.A. (1971). *Biochemistry*. **10**, 470-476.

Bryson, J.W., Betz, S.F., Lu, H.S., Suich, D.J., Zhou, H.X., O'Neil, K.T. and DeGrado, W.F. (1995). *Science*. **270**, 935-941.

Chakrabartty, A., Doig, A.J. and Baldwin, R.L. (1993a). *Proc. Natl. Acad. Sci. USA*. **90**, 11332-11336.

Chakrabartty, A., Kortemme, T., Padmanabhan, S. and Baldwin, R.L. (1993b). *Biochemistry*. **32**, 5560-5565.

Chou, P.Y. and Fasman, G.D. (1978). *Adv. Enzym. Relat. Areas Mol. Biol.* **47**, 45-148.

Cohen, B.I., Presnell, S.R. and Cohen, F.E. (1993). *Protein Sci.* **2**, 2134-2145.

Cort, J., Liu, Z., Lee, G., Harris, S.M., Prickett, K.S., Gaeta, L.S.L. and Andersen, N.H. (1994). *Biochem. Biophys. Res. Comm.* **204**, 1088-1095.

Creighton, T.E. (1993). *Proteins: Structures and Molecular Properties*. W. H. Freeman and Company, New York.

Dado, G.P. and Gellman, S.H. (1993). *J. Am. Chem. Soc.* **115**, 12609-12610.

Elöve, G.A., Chaffotte, A.F., Roder, H. and Goldberg, M.E. (1992). *Biochemistry*. **31**, 6876-6883.

Fersht, A. (1985). *Enzyme Structure and Mechanism*. W.H. Freeman & Co., New York.

- Forood, B., Perez-Paya, E., Houghten, R.A. and Blondelle, S.E. (1995). *Biochem. Biophys. Res. Comm.* **211**, 7-13.
- Glasoe, P.K. and Long, F.A. (1960). *J. Phys. Chem.* **64**, 188-190.
- Goodman, M. and Kossoy, A. (1966). *J. Am. Chem. Soc.* **88**, 5010-5015.
- Greenfield, N. and Fasman, G.D. (1969). *Biochemistry.* **8**, 4108-4116.
- Johnson, W.C. (1985). *Methods of Biochemical Analysis.* **31**, 61-163.
- Johnson, W.C. (1990). *Proteins: Structure, Function, Genetics.* **7**, 205-214.
- Kabsch, W. and Sander, C. (1984). *Proc. Natl. Acad. Sci. USA.* **81**, 1075-1078.
- Kemp, D.S., Curran, T.P., Davis, W.M. and Boyd, J.G. (1991). *J. Org. Chem.* **56**, 6672-6682.
- Kim, P.S. and Baldwin, R.L. (1984). *Nature.* **307**, 329-334.
- Kim, P.S., Bierzynski, A. and Baldwin, R.L. (1982). *J. Mol. Biol.* **162**, 187-99.
- Kumar, G.S. and Neckers, D.C. (1989). *Chem. Rev.* **89**, 1915-1925.

Lansbury, P.T. (1995). *Arzneimittel-Forschung/Drug Research*. **45-1**, 432-434.

Lesk, A.M. (1991). *Protein Architecture: A Practical Approach*. The Practical Approach Series. Oxford University Press, New York.

Lewis, J.W., Goldbeck, R.A., Kliger, D.S., Xie, X., Dunn, R.C. and Simon, J.D. (1992). *J. Phys. Chem.* **96**, 5243-5254.

Manning, M.C., Illangasekare, M. and Woody, R.W. (1988). *Biophys. Chem.* **31**, 77-86.

Marqusee, S. and Baldwin, R.L. (1987). *Proc. Natl. Acad. Sci. USA*. **84**, 8898-8902.

Marqusee, S., Robbins, V.H. and Baldwin, R.L. (1989). *Proc. Natl. Acad. Sci. USA*. **86**, 5286-5290.

Miller, M., Schneider, J., Sathyanarayana, B.K., Toth, M.V., Marshall, G.R., Clawson, L., Selk, L., Kent, S.B.H. and Wlodawer, A. (1989). *Science*. **246**, 1149-1152.

Mostad, A. and Rømming, C. (1971). *Acta Chemica Scandinavica*. **25**, 3561-3568.



Mutter, M., Gassmann, R., Buttkus, U. and Altmann, K.H. (1991).  
*Angew. Chem., Int. Ed. Engl.* **30**, 1514-1516.

Mutter, M. and Hersperger, R. (1990). *Angew. Chem., Int. Ed. Engl.*  
**29**, 185-187.

Nguyen, J., Baldwin, M.A., Cohen, F.E. and Prusiner, S.B. (1995).  
*Biochemistry.* **34**, 4186-4192.

Osterman, D.G. and Kaiser, E.T. (1985). *J. Cell. Biochem.* **29**, 57-72.

Padmanabhan, S. and Baldwin, R.L. (1994). *J. Mol. Biol.* **241**, 706-  
713.

Padmanabhan, S., York, E.J., Gera, L., Stewart, J.M. and Baldwin, R.L.  
(1994). *Biochemistry.* **33**, 8604-8609.

Pauling, L. and Corey, R.B. (1951). *Proc. Natl. Acad. Sci. USA.* **37**, 729.

Pauling, L., Corey, R.B. and Branson, H.R. (1951). *Proc. Natl. Acad. Sci.*  
*USA.* **37**, 205.

Pieroni, O. and Fissi, A. (1992). *J. Photochem. Photobiol. B.* **12**, 125-  
140.

Pieroni, O., Fissi, A., Viegi, A., Fabbri, D. and Ciardelli, F. (1992). *J. Am.*  
*Chem. Soc.* **114**, 2734-2736.

Prusiner, S.B. (1994). *Annual Review Of Microbiology*. **48**, 655-686.

Reed, J. and Kinzel, V. (1993). *Proc. Natl. Acad. Sci. USA*. **90**, 6761-5.

Rosenheck, K. and Doty, P. (1961). *Proc. Natl. Acad. Sci. USA*. **47**,  
1775-1785.

Rost, B., Sander, C. and Schneider, R. (1994). *J. Mol. Biol.* **235**, 13-26.

Schafmeister, C.E., Miercke, L.J. and Stroud, R.M. (1993). *Science*. **262**,  
734-8.

Scheraga, H.A. (1978). *Pure Appl. Chem.* **50**, 315-324.

Shoemaker, K.R., Fairman, R., Schultz, D.A., Robertson, A.D., York, E.J.,  
Stewart, J.M. and Baldwin, R.L. (1990). *Biopolymers*. **29**, 1-11.

Shoemaker, K.R., Kim, P.S., Brems, D.N., Marqusee, S., York, E.J.,  
Chaiken, I.M., Stewart, J.D. and Baldwin, R.L. (1985). *Proc. Natl. Acad.  
Sci. USA*. **82**, 2349-2353.

Shoemaker, K.R., Kim, P.S., York, E.J., Stewart, J.M. and Baldwin, R.L.  
(1987). *Nature*. **326**, 563-567.

Smallcombe, S.H. (1993). *J. Am. Chem. Soc.* **115**, 4776-4785.

Stoutland, P.O., Dyer, R.B. and Woodruff, W.H. (1992). *Science*. **257**, 1913-1917.

Taylor, J.W., Shih, I.L., Lees, A.M. and Lees, R.S. (1993). *Int. J. Pept. Protein Res.* **41**, 536-547.

Vuilleumier, S., Sancho, J., Loewenthal, R. and Fersht, A.R. (1993). *Biochemistry*. **32**, 10303-10313.

Waterhous, D.V. and Johnson, W.C. (1994). *Biochemistry*. **33**, 2121-2128.

Williams, D.H. and Fleming, I. (1980). *Spectroscopic Methods in Organic Chemistry*. McGraw-Hill, New York.

Woody, R.W. (1985). In E. Gross and J. Meienhofer (ed.), *The Peptides: analysis, synthesis, biology.*, Academic Press, Inc., New York, pp. 15-114.

Woody, R.W. (1994). *European Biophysics Journal*. **23**, 253-262.

Zagorski, M.G. and Barrow, C.J. (1992). *Biochemistry*. **31**, 5621-5631.

Zhang, C.F., Lewis, J.W., Cerpa, R., Kuntz, I.D. and Kligler, D.S. (1993). *J. Phys. Chem.* **97**, 5499-5505.

Zhang, S., Lockshin, C., Cook, R. and Rich, A. (1994). *Biopolymers*. **34**, 663-672.

Zhong, L. and Johnson, W.C. (1992). *Proc. Natl. Acad. Sci. USA*. **89**, 4462-4465.

Zimm, B.H. and Bragg, J.K. (1959). *J. Chem. Phys.* **31**, 526-535.

## **APPENDIX**

*manuscript submitted for publication, entitled*

### **Conformational Switching In Designed Peptides: The Helix-Sheet Transition**

(authors: Robert Cerpa, Fred E. Cohen, and Irwin D. Kuntz)

*The following manuscript describes, in a more concise fashion, the major topics covered in the preceding thesis. Figure and table numbers and references refer to those in the thesis.*

## ABSTRACT

**Background:** The structure adopted by peptides and proteins depends not only on the primary sequence, but also on conditions such as solvent polarity or method of sample preparation. We examined the effect that solution conditions have on the folded conformations of two peptides; one of the peptides contains the photoisomerizable amino acid p-phenylazo-L-phenylalanine.

**Results:** Spectroscopic studies indicate that these peptides switch between helical and beta sheet conformations. The switch behavior is influenced by solution conditions including pH, NaCl concentration, temperature, and peptide concentration. The peptide containing p-phenylazo-L-phenylalanine displays a spectral shift from sheet to helix upon irradiation.

**Conclusion:** We hypothesize that the structural states of the peptide are a monomeric alpha helix and an aggregated antiparallel beta sheet. Conditions encouraging aggregation tend to favor sheet; conditions discouraging aggregation tend to favor helix.

Consideration of such solution-dependent conformational changes may affect *de novo* protein design and have a bearing on certain biological processes.

## INTRODUCTION

An important goal of protein science is understanding the relationship of the amino acid sequence of a protein to its secondary and tertiary structure. Many approaches to predicting structure from sequence build upon the underlying assumption that in a given environment, a sequence will have a unique structure. While it has long been recognized that proteins and peptides exhibit an equilibrium between folded and denatured states, it is increasingly clear that many peptides can be driven to alternative *folded* structures by changing the solution conditions. Doty demonstrated the ability of polylysine to adopt different secondary structures depending on the solution environment and method of sample preparation (Rosenheck and Doty, 1961). Kabsch and Sander showed that identical pentapeptide sequences are found with different structures, depending on the protein context they occurred in (Kabsch and Sander, 1984). Cohen et al. (Cohen et al., 1993) extended this observation to hexapeptides and longer sequences. More recently, Johnson (Waterhous and Johnson, 1994; Zhong and Johnson, 1992) and Mutter (Mutter et al., 1991; Mutter and Hersperger, 1990) have explored the effects of various solvent additives to induce peptides to switch between structured states. Mutter dubbed peptides displaying dramatic, solvent-dependent conformational changes "switch peptides." Recently, attention has focused on the possibility that conformationally sensitive sequences

may play a role in diseases such as Alzheimer's dementia (Zagorski and Barrow, 1992) and prion diseases (Nguyen et al., 1995).

Switch peptides have also been created by perturbing the chemical nature of side chains (Dado and Gellman, 1993). An intriguing class of peptides utilize photoisomerizable side chains (Pieroni and Fissi, 1992). Incorporation of azobenzene, either as a side chain in the amino acid *p*-phenylazo-L-phenylalanine (Goodman and Kossoy, 1966) or by direct coupling of azobenzene derivatives to other side chains, has enabled development of several peptides displaying "photoswitch" behavior (Pieroni and Fissi, 1992). These previous studies generally relied on homopolymers of azobenzene-containing amino acids. In this paper, we explore site-specific substitution of an azobenzene amino acid in small peptides. To accomplish this goal, we synthesized Fmoc-phenylazophenylalanine for utilization in solid-phase peptide synthesis.

We report here on two peptides (Figure 2). The first was developed to model alpha helix behavior (Bradley et al., 1990). Residues with strong helix-forming potential were used (Chou and Fasman, 1978). The helical potential was enhanced by placing residues with negatively charged side chains towards the N-terminus, and residues with positively charged side chains towards the C-terminus (Shoemaker et al., 1987). Residues were also aligned to create *i, i+4* spaced salt bridges in the helical state between glutamate and lysine side chains, and the salt bridges were also aligned so as to interact favorably with the helix dipole moment (Marqusee and Baldwin, 1987). The overall amino acid content was chosen with the need for high water solubility in mind and for



convenience in assigning the proton NMR spectrum of the peptide. Tyrosine was used for convenient measurement of peptide concentration by UV absorbance.

While these design principles successfully enabled formation of an alpha helix (Bradley et al., 1990), a second design was (inadvertently) built into the peptide that favored beta sheet, not alpha helix, formation. Figure 3 illustrates how the peptide could form an amphiphilic beta sheet, with stabilizing salt bridges between adjacent strands. This is a familiar design principle, which has been exploited by other researchers (Brack and Spach, 1981; Osterman and Kaiser, 1985).

The second peptide incorporated p-phenylazo-L-phenylalanine (Goodman and Kossoy, 1966), replacing the phenol side chain of tyrosine with an azobenzene group as a side chain at position 12 in the peptide. The photoisomerizable side chain of the phenylazophenylalanine residue provides yet another variable affecting the balance between alpha helix and beta sheet. In the *trans* state of azobenzene, which tends to be the most stable conformation, the rings lie in a plane and the molecule has a very small dipole moment. The *cis* state, however, is nonplanar and has a large dipole moment (Kumar and Neckers, 1989). Because of the helix-stabilizing interactions between the tyrosine at position 12 and the histidine at position 16 in the parent peptide (Bradley et al., 1990), the tyrosine was replaced with phenylazophenylalanine in anticipation of a significant perturbation upon photoisomerization of the side chain.

Given the potential to form two extremely different ordered structures, alpha helix and beta sheet, we investigated the effect that different conditions have on the structure that the peptides adopt.

## RESULTS

*pH titration.* Circular dichroism spectra of the pH titration of peptide I, at 100  $\mu$ M peptide concentration, are shown in Figure 10; the mean residue ellipticity at 222 nm is plotted versus pH in Figure 11. The buffer solution contains 100 mM NaCl and 1 mM each of sodium citrate, phosphate, and borate. The peptide spectra are typical of partially helical peptides, displaying two minima at approximately 222 nm and 205-208 nm with an isosbestic point at 203 nm. The helical signal increases slightly from pH 2 to 4, and then drops rapidly from pH 4 to 5, continuing to decrease smoothly as the pH increases.

Increasing the peptide I concentration to 1.2 mM results in much different behavior. The peptide displays helical spectra at pH 2 (Figure 12) and 3 (not shown). However, at pH 5, the spectrum is most suggestive of beta sheet structure (a single minimum at 218 nm) and the peptide solution was cloudy (Figure 12). At higher pH's, the spectra have a single minimum that is significantly red-shifted; the position of the UV maximum is also red-shifted (Figure 13). Large amounts of precipitate were visible above pH 5; distortions due to light scattering may be affecting the spectra. Dropping the pH

from 8 to 2 restored the alpha helical spectrum and caused most of the precipitate to re-dissolve (Figure 13).

Circular dichroism at selected pH values for peptide II, at 300  $\mu\text{M}$  peptide concentration, also demonstrate alpha helical spectra at low pH and conversion to beta sheet at higher pH, as shown in Figure 17. These spectra were taken in distilled water, as peptide II structure is affected by NaCl concentration (see below). The alpha-to-beta transition in peptide II can also be reversed by returning the solution to acidic pH.

*Salt concentration effects.* The conformation of peptide II is also affected by NaCl concentration. Figure 18 shows the CD spectra of peptide II in 10 mM sodium phosphate, with and without 100 mM NaCl added, at 900  $\mu\text{M}$  peptide concentration. In Figure 19, spectra taken at intermediate concentrations of salt are displayed. The solutions were prepared in  $\text{D}_2\text{O}$ ; the pH\* was 2. Increasing salt concentration causes a smooth increase in the amount of beta sheet character in the spectrum. In Figure 21, IR spectra of peptide II with and without salt present show a clear shift in the amide I' band. The sample containing salt shows an amide I' absorption peak at  $1612\text{ cm}^{-1}$ , a region assigned to low-frequency beta sheet. When no salt was present in the sample, the amide I' peak occurs at approximately  $1650\text{ cm}^{-1}$ , in the alpha helix/random coil region.

*Temperature effects.* Heating a solution of peptide II (peptide concentration of 75  $\mu\text{M}$ ) in a buffer solution containing 100 mM NaCl yields the temperature denaturation curves shown in Figures 22 and 23. Even at  $70^\circ\text{C}$ , there is a significant dip in the CD curve at 220 nm; this may be due to the intense UV transition of the azobenzene

side chain in this region, although there may also be residual beta-sheet structure. After cooling the heated solution back to 5°C, the spectrum displays the characteristics of an alpha helix. Over several months' time, the spectrum gradually changes back to the single-minimum spectrum characteristic of beta sheet.

*Concentration effects.* CD spectra of peptide II in 100 mM NaCl buffer solution at different peptide concentrations are shown in Figure 28. At the two higher concentrations, 375  $\mu$ M and 75  $\mu$ M peptide (at pH 2.3), the spectra have the single minimum at 218 nm characteristic of beta sheets. However, at the lowest concentration, 7.5  $\mu$ M peptide (pH 2.2), the spectrum has the double-minima appearance of an alpha helix.

*Photoisomerization effects.* The CD spectra of 75  $\mu$ M peptide II are shown before and after irradiation with ultraviolet light (Figure 29). The peptide displays a single-minimum curve characteristic of beta sheet prior to exposure to UV light. After the 1-hour irradiation, the CD spectrum of the peptide displays the double-minima curve typical of helix. Storing the peptide solution in the dark does not reverse the transition, even after several weeks time, unlike the behavior described above for peptide II after heating.

*Nuclear magnetic resonance spectra.* The fingerprint and amide regions of the NOESY spectrum of peptide I are shown in Figures 31 and 32, respectively. Resonance assignments are shown in Table I and are referenced to TSP. The spectrum is typical of helical peptides, as seen in the summary of observed NOEs in Figure 33, and is virtually identical to the spectrum found for a related peptide studied under similar conditions (Bradley et al., 1990).

Fingerprint and amide regions of peptide II are shown in Figures 34 and 35, and residues with chemical shifts displaced by more than 0.05 ppm from their counterparts in peptide I are summarized in Table II. (The side chains of the lysines and of Thr-4 and Leu-9 could not be traced unambiguously in the NOESY spectrum because of the low peptide concentration needed to prevent aggregation.) Of the amino acids common to both peptides I and II, only His-16 resonances are displaced by more than 0.1 ppm. Since the side chain of His-16 is in an  $i, i+4$  arrangement to the azobenzene side chain of Z-12, a change in the environment (and the chemical shifts) of the histidine is expected from the tyrosine to phenylalanylalanine mutation. The spectrum of peptide II contains fewer of the characteristic helical NOESY peaks expected, as shown in Figure 36. However, the lack of any significant difference between the chemical shifts of peptides I and II, combined with the helical NOEs observed for peptide II, indicates that peptide II is significantly helical under the conditions studied.

In summary, both peptides display more beta sheet character at higher peptide concentrations, higher NaCl concentrations, and at pH values of 5 or higher. Heating or photoisomerization of the azobenzene chain in peptide II disrupts the beta sheet character of the spectra.

## **DISCUSSION**

The dramatic changes in the spectra of the peptides under different conditions strongly suggest that the peptides are undergoing structural transitions. The conformational states proposed for the peptides--an intermolecular beta sheet and a monomeric alpha helix--are discussed below. These conformations provide a straightforward and consistent rationale for interpreting CD and IR experiments as a function of peptide concentration, salt concentration, pH, and temperature, as well as the change in the CD spectrum observed upon ultraviolet irradiation of peptide II. We also consider experimental artifacts that might complicate this interpretation.

We start by examining the hypothesis that the structural states we observe are an intermolecular beta sheet aggregate (see Figure 3), and a monomeric helix. The similar spectra and characteristic helical NOEs observed in the NMR experiments on peptides I and II (Figs. 31-36), as well as in the parent peptide studied earlier (Bradley et al., 1990), clearly support an alpha helical conformation at low pH and low salt conditions. The CD experiments as a function of peptide concentration support the hypothesis that the beta sheet state arises due to aggregation: alpha helix is stable at lower concentration, while the beta sheet spectra are observed at higher concentrations where aggregation is more likely. A similar antiparallel beta sheet aggregate structure has been proposed for an amphiphilic peptide that forms a highly stable beta sheet (Zhang et al., 1994).

This model also accounts for the results observed in the experiments in which pH and salt concentrations are varied. The pH

titration of peptide I at 1.2 mM concentration suggests that the peptide forms an alpha helix at pH 2, where the peptide carries a net charge of +4, which would disfavor aggregation. As the pH rises and the glutamic acid residues begin to deprotonate, the alpha helical spectrum becomes distorted (data not shown); at pH 5, where most of the glutamic acid residues are negatively charged, the peptide carries a net charge of +1 and has less electrostatic repulsion to overcome to aggregate. This aggregation event occurs at much lower concentration in peptide II than in peptide I. At 100  $\mu$ M peptide concentration and 100 mM NaCl concentration, peptide I displays a (partially) helical conformation at all pH values. Peptide II, however, gives rise to a beta sheet CD spectrum at 75  $\mu$ M peptide concentration at pH 2.3, 100 mM NaCl concentration.

The aggregated beta sheet/monomer alpha helix model also provides a straightforward explanation of the NaCl titration results and heating experiment. Peptide II, like peptide I, has a net charge of +4 at low pH. Increasing the amount of salt present in solution screens the charge on the peptide more effectively, facilitating formation of the aggregated beta sheet as observed in Figures 18 and 19. Similarly, heating the peptide II solution could lead to disaggregation of the beta sheet complex into extended monomers at higher temperatures. Upon cooling, the peptide would adopt the preferred monomeric conformation of alpha helix.

The conformations of peptide I and peptide II are influenced by a wide variety of solution conditions. The fact that a single peptide can adopt two very different secondary structures based on the solution environment carries important implications for biological

systems and for protein design and engineering. Earlier work has shown that peptide conformation is affected by solution additives such as trifluoroethanol and sodium dodecyl sulfate (Mutter and Hersperger, 1990; Reed and Kinzel, 1993; Waterhous and Johnson, 1994; Zhong and Johnson, 1992) and interface effects (Taylor et al., 1993). In the experiments presented here, we show that peptide concentration, pH, and salt concentration also play a role in determining peptide structure. From a biological perspective, the most significant of these factors are the pH and salt concentration; physiological systems often contain environments of different ionic strength or pH separated by membranes, which may influence peptide and protein structures in those environments. The salt concentrations used here are well within the limits encountered in living systems (ca. 150 mM (Alberts et al., 1994)). Understanding how and why peptides aggregate may have important biological implications, as the conversion of an alpha helical peptide or protein into an aggregated, insoluble beta sheet form may be a factor in the pathology observed in Alzheimer's disease and prion diseases (Nguyen et al., 1995; Zagorski and Barrow, 1992).

The photoswitch behavior of peptide II is of distinct interest, since it enables the study of a conformational switch triggered by the rapid *trans*-to-*cis* azobenzene photoisomerization. Other peptides containing phenylazophenylalanine (Goodman and Kossoy, 1966) or azobenzene (Pieroni and Fissi, 1992) side chains have been studied; many of these peptides also display changes in secondary structure upon irradiation. An important difference should be noted between the previous systems and the peptide studied here which renders



peptide II particularly useful. The systems used in previous experiments were typically high molecular weight polymers, with a large percentage of azobenzene incorporated into each peptide chain. In contrast, peptide II is relatively short and contains only one azobenzene residue, making it much more feasible to study the peptide and to examine the effects of replacing individual residues on the structural transition.

An important caveat that must be considered in any interpretation of our results is the possibility that spectral artifacts, not true conformational transitions, account for the beta sheet and alpha helix spectra. Aromatic residues, such as tyrosine and tryptophan, are known to distort the circular dichroism spectra of peptides and proteins, due to overlap of electronic transitions from the peptide bonds and the aromatic rings (Chakrabartty et al., 1993b; Vuilleumier et al., 1993). The azobenzene side chain has particularly strong electronic transitions in the peptide bond region, which requires caution in interpreting CD spectra. Infrared spectroscopy utilizes a different physical property of the peptide bond than CD, making it unlikely that artifacts will be mistaken for true conformational changes in both types of spectra. The weak azobenzene stretching frequency occurs outside of the amide I' region, and is unlikely to affect the results of the FTIR experiments (Williams and Fleming, 1980). The experiments with the peptides at different concentrations also lends support to the aggregate/monomer hypothesis. Since the concentration of the peptides dramatically affects the spectrum obtained, the CD spectra almost certainly arise from a true aggregation event, not from

artifacts due to the aromatic side chains. Finally, NMR provides yet another independent physical method of determining conformation, and the strongest evidence for the helical state of the peptides. Attempts at acquiring NMR spectra using the beta sheet-forming conditions were unsuccessful due to extremely broad linewidths (data not shown). While this prevents solution NMR structure determination under those conditions, it also provides another piece of evidence that an aggregation event is occurring during the structural transition.

Two interesting aspects of the CD spectra presented here merit comment. The first aspect is the relative intensity of the minima of helix and sheet in Figures 12, 13, 17, 18, 23, 24, 28, and 29. The spectrum of an alpha helix tends to have a minimum approximately twice as strong as a beta sheet spectrum, as observed in the pure component spectra for polylysine (Greenfield and Fasman, 1969). The spectra of alpha helix and beta sheet presented here have roughly equal intensities at their minima. A reasonable explanation for this phenomenon is that the beta sheet conformation places a larger percentage of the peptide bond chromophores in ordered secondary structure than the alpha helical conformation. It is also possible that the azobenzene electronic transitions discussed above, while not strong enough to distort the qualitative information contained in the CD spectra, affect the magnitude of the spectra associated with alpha helix and beta sheet. A second unusual aspect of the CD spectra is observed in Figure 13, where both the  $n-\pi^*$  and  $\pi-\pi^*$  transitions of the beta sheet spectra observed at pH 6 and 8 are red-shifted, and the intensity of the  $\pi-\pi^*$  transition of the sheet at pH

8 is stronger than that of the same transition in the alpha helix. Such a red shift and enhanced intensity have been calculated for model polyvaline beta sheet spectra (Manning et al., 1988), and are attributed to the strong twist in the sheet caused by the beta-branched side chains of valine. It is possible that the presence of the three threonine residues are causing similar phenomena to occur in our spectra. Other researchers have also noted unusually high intensity for the  $\pi$ - $\pi^*$  transition in beta sheets, although the maxima were blue-shifted (Cort et al., 1994).

The data presented here add to the diversity of conformational behavior observed in peptides. Our peptide design provides an excellent system for studying beta sheet-alpha helix conformational switching. Mutation of residues can illuminate the dependence of the conformational switching behavior on specific amino acids. Experiments with a variety of salts and solution additives can yield thermodynamic data for the conformational switch under different solution conditions. Finally, the photoswitch behavior of peptide II can be utilized for studying the kinetics of secondary structure interconversion. Rapid spectroscopic techniques have been developed which can detect such changes on nanosecond (Zhang et al., 1993) and picosecond (Lewis et al., 1992; Stoutland et al., 1992) time scales; studies utilizing peptide II in this area are underway.

## **MATERIALS and METHODS**

### *Peptide Synthesis and Purification*

Peptides were synthesized on an Applied Biosystems, Inc. (ABI) Model 431A peptide synthesizer using Fmoc (9-fluorenylmethoxycarbonyl) chemistry. Benzotriazolyl tetramethyluronium hexafluorophosphate (HBTU)/hydroxybenzotriazole (HOBt) coupling reagents were used for peptide I; dicyclohexylcarbodiimide/HOBt coupling reagents were used for peptide II. Double coupling of standard Fmoc amino acid residues was employed. Standard Fmoc amino acids were purchased from Millipore; reagents were purchased from ABI and Aldrich, and solvents from ABI or Baxter. The procedure of Goodman and Kossoy (Goodman and Kossoy, 1966) was used to synthesize p-phenylazo-L-phenylalanine, and the Fmoc derivative was synthesized using fluorenylmethylsuccinimidyl carbonate (Aldrich) (Atherton and Sheppard, 1989). Millipore PAL Resin was used to generate carboxy-terminal amide groups, and the amino terminus was acetylated. Peptide I was cleaved using 95% trifluoroacetic acid/3% anisole/1% ethanedithiol/1% thioanisole. After 90 minutes, the solution was filtered, the volume reduced by evaporation, and the peptide was precipitated by adding cold ether. The precipitate was redissolved in distilled H<sub>2</sub>O, and lyophilized. Peptide II was cleaved with 80% trifluoroacetic acid/8% anisole/4% ethanedithiol/4% thioanisole. As peptide II tended to form an oil upon addition of ether to the TFA solution, the cleavage solution was evaporated and the excess scavengers separated from the colored peptide oil by pipette. The oil was then redissolved in distilled H<sub>2</sub>O and lyophilized.

The crude peptides were purified by reverse-phase HPLC on Vydac C-18 semipreparative columns using a water/acetonitrile gradient containing 0.1% TFA, monitoring elution at either 275nm (peptide I) or 325nm (peptide II). Peptide I was subjected to a second purification on a Vydac C-4 semipreparative column using water/acetonitrile/TFA solvents. The identity of the purified peptides was established by FAB mass spectrometry (peptide I, MH+ 1945.3 calc., 1945.1 found; peptide II, MH+ 2033.1 calc., 2033.3 found; the sodium adduct was also observed in both cases). Peptide purity was assayed by HPLC on a Vydac C-18 analytical column, with detection at 215 nm. Peptide I was 94% pure; peptide II was 99% pure and consisted of an 8:1 mixture of *trans:cis* isomers of the phenylazophenylalanine side chain (the peak consisting of pure *trans* isomer was isomerized on passage through the HPLC UV detector).

### *Circular Dichroism*

Circular dichroism (CD) on peptide II was carried out on a Jasco J-500 spectrometer. Circular, temperature-controlled cuvettes were used. CD on peptide I was performed on a Jasco J-710 spectrometer; rectangular cells and a Peltier temperature control unit were employed. A baseline spectrum was subtracted from the sample spectrum unless noted otherwise. In the spectra collected in rectangular cells, the region near 260 nm, while flat, often was offset from zero even after baseline correction; this region was set to zero by subtracting the average of the data from 256 nm to 260 nm. No smoothing was performed on the CD spectra.

### *Fourier Transform Infrared Spectroscopy*

Fourier transform infrared spectra of peptide II were collected on a Perkin-Elmer System 2000 FTIR microscope. A 50  $\mu\text{m}$  path cell with calcium fluoride windows was used. The HPLC-purified peptide was lyophilized at least twice out of 20 mM HCl solution to remove traces of TFA, then lyophilized once from D<sub>2</sub>O solution. The dry deuterated peptide was then taken up in D<sub>2</sub>O buffers immediately before acquiring spectra; pH\* of solutions was measured after acquiring spectra. Spectra of the buffers were also acquired under identical conditions and subtracted from the peptide spectra. Residual water signal was removed by linear interpolation across the narrow-linewidth water peaks. The spectra were smoothed and the amide I' region was fitted to a flat baseline; no self-deconvolution was used.

### *Ultraviolet Irradiation*

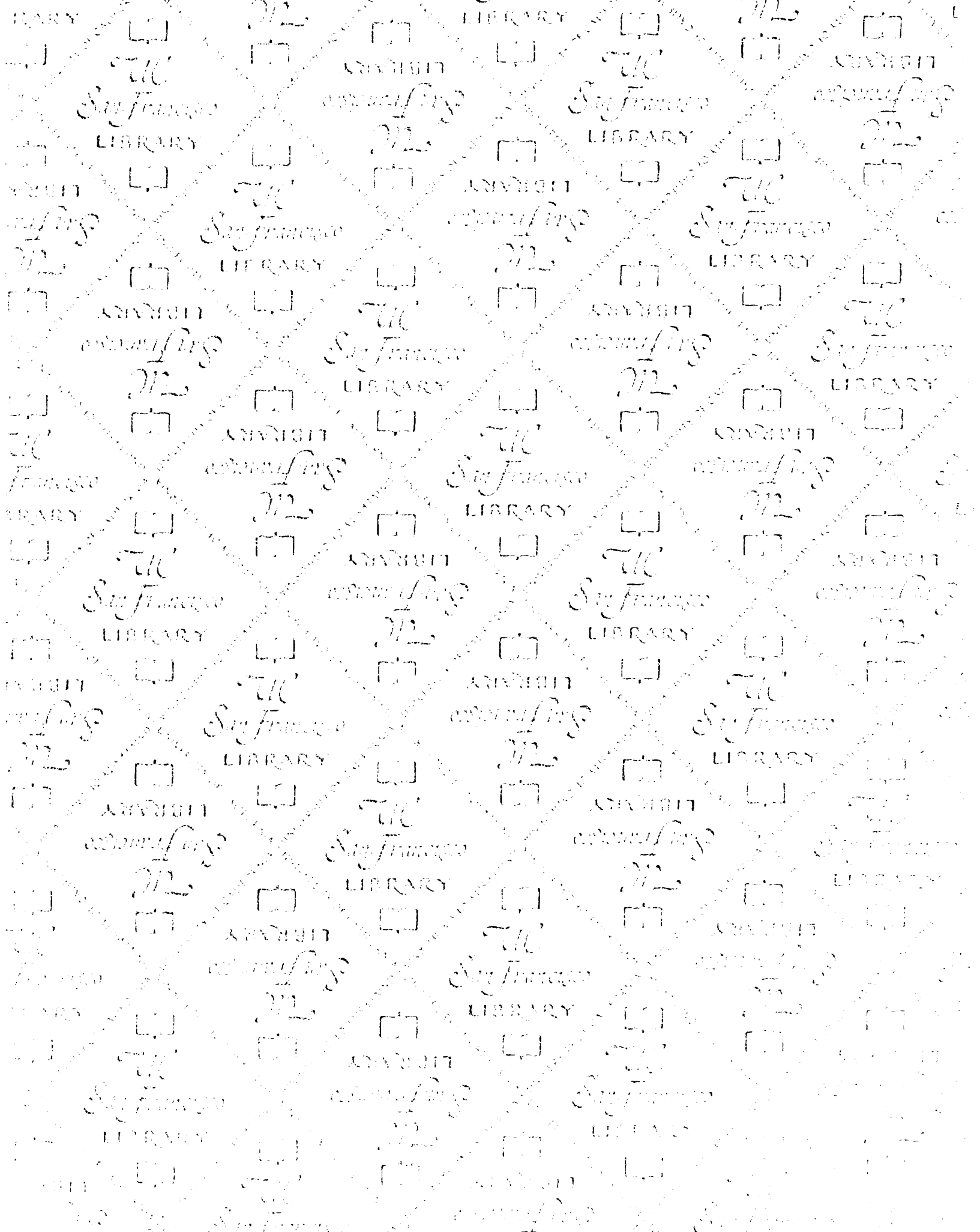
Peptide II solution (75  $\mu\text{M}$  peptide) was placed in a glass cell and the cell was placed in a Pyrex beaker containing water and ice (replenished periodically) to prevent heating of the sample. The beaker was then placed a few inches from a medium pressure Hanovia L679A 450 W lamp (equipped with a Pyrex glass shield to remove short-wavelength light) for 60 minutes. CD spectra were then acquired within 10 minutes after ending irradiation.

## *Nuclear Magnetic Resonance Spectroscopy*

NOESY, COSY, and HOHAHA spectra of peptide I in 90% H<sub>2</sub>O/10% D<sub>2</sub>O at 15°C, 5 mM peptide concentration, pH 2.4, were recorded on a General Electric 500 MHz Omega system, using presaturation to suppress the water signal. A NOESY spectrum of peptide II in 90%H<sub>2</sub>O/10%D<sub>2</sub>O was recorded on a Varian Unity 600 MHz spectrometer at 15°C, 460 μM peptide concentration, pH 2.4, using a 10 mm probe; symmetrically-shifted pulses were used for water suppression (Smallcombe, 1993). A mixing time of 150 msec was used for the NOESY spectra. The spectra were processed using software developed at UCSF by M. Day and D. Kneller (unpublished).

### **ACKNOWLEDGEMENTS**

The assistance of Dallas Connor, Joe Zhou, and Profs. Martin Shetlar, Lech Celewicz, and Phyllis Kosen is gratefully acknowledged. Robert Cerpa was a Howard Hughes Medical Institute Predoctoral Fellow and a University of California Presidential Dissertation Year Fellow. The UCSF Computer Graphics Lab is supported by NIH grant P41-RR01081. The UCSF Mass Spectrometry Lab (A.L. Burlingame, Director) is supported by the Biomedical Research Technology Program of the National Center for Research Resources, NIH NCRR B RTP 01614. This research was supported by NIH grants GM-19267, GM-39900 and AG-02132.





# For reference

Not to be taken from the room.

6462959



3 1378 00646 2959

